NATIONAL ADVISORY COMMITTEE FOR AERONAUTICS

TECHNICAL MEMORANDUM 1390

ON THE MECHANISM OF BUCKLING OF A

CIRCULAR CYLINDRICAL SHELL UNDER AXIAL COMPRESSION

By Y. Yoshimura

Washington

July 1955

NATIONAL ADVISORY COMMITTEE FOR AERONAUTICS

TECHNICAL MEMORANDUM 1390

ON THE MECHANISM OF BUCKLING OF A CIRCULAR CYLINDRICAL SHELL UNDER AXIAL COMPRESSION[1]

By Y. Yoshimura[2]

INTRODUCTION

Ever since A. Robertson (ref. 1), E. E. Lundquist (ref. 2), and L. H. Donnell (ref. 3), showed that the experimental buckling load of a circular cylindrical shell under axial compression is much smaller than the theoretical value much effort has been devoted to this problem. Among the more recent theories, the nonlinear finite deformation theory given by Th. von Kármán and Hsue-Shen Tsien (ref. 4) and T. Kono (ref. 5) explains convincingly the discrepancy between the experimental and theoretical buckling load hitherto computed by the classical theory, and the large and abrupt displacement and the decrease of load in buckling.

The stress-strain relationship obtained by Von Kármán, etc., certainly indicates an important feature of the buckling of a circular cylindrical shell. However, the idea that the minimum value of the load given by the load-deflection curves may be realized is not considered appropriate.[3] The state which may be actually realized after buckling must be determined by minimizing the energy, not only with respect to the magnitude of deflection, but also to the aspect ratio and the circumferential number of buckling waves. The actual buckling load will be given by a comparison of energy levels before and after buckling and the energy barrier to be jumped over in buckling.[3] Based on such a concept, the general buckling and the local buckling of a cylindrical shell are considered to be quite different phenomena from the energy viewpoint, though they are equivalent with respect to the load.

---

[1] After this investigation was performed, the author became aware of Professor H. S. Tsien's paper "A Theory for the Buckling of Thin Shells", Journ. Aero. Sci. 9, 1942, 373-384, which had remained unknown to us due to the war.

[2] Associate Professor of University of Tokyo.

[3] Note by reviewer: The energy level concept was also clarified by Von Kármán and Tsien in the paper quoted above.

The reason why the cylindrical shell reveals such a particular behavior for buckling will be attributed to the geometrical features of its deformation, that is, to the fact that a developable surface quite different from the original cylindrical surface can exist. On the basis of these fundamental concepts concerning deformation and energy, the mechanism of the buckling can be understood more completely.

LIST OF SYMBOLS

a	radius of cylinder
e	axial shortening per unit axial length
e_o, e^* e_1, e_{cr}	see figure 7
e_{11}, e_{12} e_{22}	components of membrane strain
e'	$= \epsilon'/\sqrt{\alpha}$
f_{ij}	$= \delta_j/a$ = coefficients of Fourier series, equation (10)
g_1, g_2	defined by equation (24)
h	see figure 3
k	aspect ratio of buckles = l_y/l_x
l_x	length of buckle in axial direction
l_y	length of buckle in circumferential direction
l_x'	see figure 3
n	number of circumferential waves
p	see figure 3
q	dimensionless critical loading = $\frac{\sigma}{E\sqrt{\alpha}}$

t	thickness of cylinder wall
u, v, w	components of displacement of a point on the middle surface of the shell
x	coordinate in axial direction
y	coordinate in circumferential direction
A, B, C, D F, G, H, Q	coefficients, see equations (35), (36)
A', B', C' Q'	coefficients, see equations (37), (38)
A'', B'', C'' Q''	coefficients, see equations (60), (61)
E	Young's modulus
E_s	elastic constant of loading spring
E, F, G	coefficients of the first fundamental form of the deflection surface
L, M, N	coefficients of the second fundamental form of the deflection surface
K	Gaussian curvature
L	length of cylinder
R_1, R_2	radii of curvature of deflection surface
S, S', R T'	see figure 7
T_{11}, T_{12} T_{22}	membrane stress components

W, W_e, W_b — total extensional and bending strain energy, respectively

W', W_1', W_2' — see equation (56)

α $= \dfrac{t^2}{12(1 - \nu^2)a^2}$

δ $= a - h$

δ' $= \rho - a$

ϵ' axial shortening of cylinder per unit length

λ $= \dfrac{2\pi a}{2l_x}$

μ $= n$

ρ $= g_2/g_1$, see equation (43)

ν Poisson's ratio

σ axial compressive stress

η $n^2\sqrt{\alpha}$

Π, Π_e', Π_b — dimensionless strain energy, see equation (32)

Π', Π_1', Π_2' — dimensionless strain energy, see equation (57)

χ stress function for the membrane stress

EXPERIMENTAL RESULTS ON ELASTIC BUCKLING

As for the buckling load of a cylindrical shell, the existing results appear sufficient for the present. But it will be useful from theoretical considerations to obtain experimental data concerning the difference between the so-called buckling load and the load after buckling, the characteristics of the buckling deformation, and the effect of the rigidity of the loading equipment etc.

To clarify the post-buckling behavior, experiments were carried out with celluloid cylinders. The results are shown in figure 1 for three kinds of rigidities of loading springs. It will be needless to say that the value of q at buckling is much smaller than the value $q = 2$ of the classical theory. For cylinders whose dimensions are shown in the figure, the post-buckling load is about one third of the buckling load. The circumferential number of lobes ranges from the value 5 to 7, and their aspect ratio from 0.65 to 1.0. From the comparison of the three experiments, we can deduce that, with the increase of the rigidity of the spring, (1) both the buckling and the post-buckling load increase, (2) the value of k decreases, that is, the buckling wave form becomes more slender in the axial direction, and (3) the circumferential number of waves n increases. When the axial shortening is reversed, the load is kept nearly constant, and the value of k decreases, i.e., the wave length of the buckling lobe becomes longer, under the constant value of n. Such a change of the wave form will be proved theoretically reasonable later.

CHARACTERISTICS OF BUCKLING DEFORMATION

As for the buckling deformation of a cylindrical shell, there are two remarkable characteristics, other than those of the wave number and the aspect ratio of the lobes. The first is that the cylinder practically always buckles locally, at least in comparatively long cylinders as used in our experiments. The longitudinal range over which such buckling occurs extends over 1.5 times the axial wave length of the lobe; while circumferentially, it extends over the whole cylinder only under the condition of complete rotational symmetry of both the cylinder and the loading equipment. As will be considered later, the local buckling is attributed to the energy condition.

The second characteristic is that the buckled surface, which is greatly displaced from the initial cylindrical surface, is nearly developable. That is, the buckled surface is a regular repetition of the polygon ABCD (fig. 2), the ridges AB, BC, CD and DA and the trough BD being all nearly straight, and the surface ABD and BCD nearly

plane. Accordingly, the buckled surface is approximately a concave polyhedron constructed by connecting nearly plane triangles such as ABD. Consequently, the Gauss curvature

$$K = \frac{1}{R_1 R_2} \tag{1}$$

is vanishingly small throughout the deformed surface, where R_1 and R_2 denote the principal radii of curvature. Denoting the fundamental metrics of the first and the second kinds of the deformed middle surface by E, F, G and L, M, N, respectively, the compatibility condition is given by Gauss' characteristic equation

$$\left.\begin{aligned} \frac{1}{2}\left[2\frac{\partial^2 F}{\partial x \partial \theta} - \frac{\partial^2 E}{\partial \theta^2} - \frac{\partial^2 G}{\partial x^2}\right] &= LN - M^2 = KH^2 \\ H^2 &= EG - F^2 \end{aligned}\right\} \tag{2}$$

under the neglection of the second order terms regarding the derivatives of E, F, G. The left hand side of equation (2) is considered to be small, and as equation (2) is satisfied by the undeformed initial surface, on which the Gauss curvature vanishes completely, the expression of the left-hand side of equation (2) vanishes also for the initial surface. Consequently, when the deformed surface of the circular cylinder is nearly developable as in the case of buckling under axial compression, the deformation can be said to be almost inextensional. The deviation of the buckled middle surface from the complete developable surface will depend on the thickness of the shell. For a limiting case where the thickness tends to zero, i.e., for an ideal membrane, the buckled surface is supposed to become a complete concave polyhedron.

In case a completely developable surface is realized, the cross section through the point A in figure 2 will form a regular polygon as is shown in figure 3(a). Assuming the polygon to be n-sided, then the length of each side is $2\pi a/n$, because the deformation is completely inextensional. Hence, from the figure

$$h = \frac{\pi a}{n} \cot \frac{\pi}{n} \fallingdotseq a\left(1 - \frac{\pi^2}{3n^2}\right)$$

and the displacement at the trough is given by

$$\delta = a - h = a\frac{\pi^2}{3n^2} \tag{3}$$

Since

$$p = \frac{\pi a}{n} \operatorname{cosec} \frac{\pi}{n} \fallingdotseq a\left(1 + \frac{\pi^2}{6n^2}\right)$$

the displacement at the peak is

$$\delta' = p - a = a\,\frac{\pi^2}{6n^2} \tag{4}$$

Putting the aspect ratio k of a buckling lobe which has the wave lengths $2l_y$ and $2l_x$ in the circumferential (y) and axial (x) directions by

$$k = \frac{l_y}{l_x} \tag{5}$$

we have

$$l_x = \frac{\pi a}{nk} \tag{6}$$

by $l_y = \pi a/n$. As we have

$$l_x' = \sqrt{l_x^2 - (\delta + \delta')^2}$$

From figure 3(b), which shows the axial section of the deformed cylinder through A in figure 2, the axial shortening ϵ of the cylinder per unit axial length is given by

$$\epsilon = \frac{l_x - l_x'}{l_x} \fallingdotseq \frac{1}{2}\frac{(\delta + \delta')^2}{l_x^2}$$

and hence, from equations (3), (4) and (6),

$$\epsilon = \frac{\pi^2}{8}\,\frac{k^2}{n^2} \tag{7}$$

From equation (7), it is seen that the axial shortening of the cylindrical membrane, due to the geometrical deformation, increases as the lobe becomes flatter in the axial direction and the circumferential wave number decreases. Although the compressive load required for such a buckling into a completely developed surface vanishes, it does not vanish for an actual shell owing to deviation of the actual deformation surface from

being completely developable because of its bending rigidity. The fact that a relation similar to equation (7) holds also for the shell, as will be shown later, is considered to be an evidence for the buckled surface to be approximately developable.

The experimental fact above-mentioned, that the buckled surface of the cylindrical shell is approximately developable, is verified from the following theoretical consideration. If the higher order terms are neglected in the expression of L, M, N, with respect to derivatives of displacement components, it follows that

$$L = \frac{1}{a} w_{xx} \qquad M = w_{xy} \qquad N = a \left(1 + w_{yy}\right) \tag{8}$$

where we write w, x, y instead of w/a, x/a, y/a, respectively. If, in the following calculation, one likewise puts u, v in place of u/a, v/a, to make all quantities dimensionless, then by equation (2)

$$K = \frac{1}{a^2} \left[w_{xx} \left(1 + w_{yy}\right) - w_{xy}^2 \right] \tag{9}$$

To express the almost developable surface as shown in figure 2 by the displacement w, it is necessary to take a comparatively large number of terms of the Fourier series

$$w = \sum f_{ij} \cos i\lambda x \cos j\mu y \tag{10}$$

where

$$f_{ij} = \frac{\delta_{ij}}{a} \tag{11}$$

δ_{ij} denoting the deflection of each component of deformation, and

$$\lambda = \frac{2\pi a}{2l_x} \qquad \mu = \frac{2\pi a}{2l_y} = n \tag{12}$$

n being the circumferential wave number.

As a simple case of equation (10), if we assume

$$w = f_o + f_1 \cos \lambda x \cos \mu y + \frac{1}{2} f_2 \left(\cos 2\lambda x + \cos 2\mu y\right) \tag{13}$$

which is nothing but a wave pattern

$$\cos \lambda x \cos \mu y$$

which has the nodal lines parallel to the x- and y-axes, superimposed by a wave pattern

$$\cos (\lambda x + \mu y) \cos (\lambda x - \mu y)$$

which has the nodal lines parallel to a line having an angle $\pm \arctan \frac{\lambda}{\mu}$ with the x-axis, then we have

$$a^2 K = \lambda^2 \left(2 f_1 f_2 \mu^2 - f_1\right) \cos \lambda x \cos \mu y +$$

$$\lambda^2 \left(\frac{1}{2} f_1^2 \mu^2 - 2 f_2\right) \cos 2\lambda x + \frac{1}{2} f_1^2 \lambda^2 \mu^2 \cos 2\mu y +$$

$$4 f_2^2 \lambda^2 \mu^2 \cos 2\lambda x \cos 2\mu y +$$

$$f_1 f_2 \lambda^2 \mu^2 (\cos \lambda x \cos 3\mu y + \cos 3\lambda x \cos \mu y) \qquad (14)$$

Only the first and second terms in equation (14) can be made vanishing, and, if we choose the values of f_1 and f_2 so as to make these terms zero, it follows that

$$f_1 = \frac{\sqrt{2}}{n^2} \qquad f_2 = \frac{1}{2n^2} \qquad (15)$$

It is noteworthy that equation (15) has a form quite similar to equation (3). It is assumed in the above derivation that the series (13) has only three terms, and a choice of f_1 and f_2 is made which makes K as small as possible. If we apply the infinite series (10) generally, there exist the values

$$f_{ij} = \frac{g_{ij}}{\mu^2} \qquad g_{ij} = \text{const.} \qquad (16)$$

which make K equal to 0 completely. Therefore, the number of terms of the series must be increased, as the thickness of the shell decreases, and, for the limiting case of the ideal membrane, it will be necessary to take an infinite series.

For a flat plate, the Gauss curvature K of the deflection surface cannot vanish unless all the coefficients f_{ij} vanish, by reason of non-existence of the term w_{xx} in the right-hand side of equation (9). This shows that no developable surface exists in flat plates other than the initial plane, contrary to the case of the circular cylindrical shell. Consequently, when a flat plate performs finite displacement, severe bending must be accompanied with large extension of the middle surface. This is the reason why a flat plate and a cylindrical shell exhibit substanially different behaviors during buckling.

GENERAL BUCKLING

Actual buckling is local in all cases, as was described in the last paragraph, except when a cylinder has a particular length. However, in order to treat the local buckling, it is first necessary to investigate the phenomenon of general buckling.

Before proceeding to the subject, it is necessary to prove the existence of the stress function even in the state of large deformation after buckling, because it has hitherto been proven only for small deformations The existence of the stress function has usually been considered to mean that the third and fourth terms can be neglected as compared with the first and second terms in the first and second equations of the equilibrium equations (ref. 6)

$$\left.\begin{aligned}
&\frac{\partial T_{11}}{\partial x} + \frac{\partial T_{12}}{\partial y} - T_{13}L - T_{23}\frac{M}{a} = 0 \\
&\frac{\partial T_{12}}{\partial x} + \frac{\partial T_{22}}{\partial y} - T_{13}\frac{M}{a} - T_{23}\frac{N}{a^2} = 0 \\
&\frac{\partial T_{13}}{\partial x} + \frac{\partial T_{23}}{\partial y} + T_{11}L + 2T_{12}\frac{M}{a} + T_{22}\frac{N}{a^2} = 0
\end{aligned}\right\} \qquad (17)$$

Physically this concept means that bending can be neglected against extension, and that the equations are satisfied for the usual extensional deformation. For the almost inextensional finite deformation, however, the existence of the stress function cannot be readily concluded in a similar manner, because T_{11}, T_{12} and T_{22} are small, and L, M, and N

large after buckling. Nevertheless, it can be derived by some other reasoning when the deformed surface remains developable.

Solving the first and second equations in (17) with respect to T_{13} and T_{23}, we have

$$\left.\begin{aligned} T_{13}\frac{LN - M^2}{a^2} &= -\frac{M}{a}\left(\frac{\partial T_{12}}{\partial x} + \frac{\partial T_{22}}{\partial y}\right) + \frac{N}{a^2}\left(\frac{\partial T_{11}}{\partial x} + \frac{\partial T_{12}}{\partial y}\right) \\ T_{23}\frac{LN - M^2}{a^2} &= L\left(\frac{\partial T_{12}}{\partial x} + \frac{\partial T_{22}}{\partial y}\right) - \frac{M}{a}\left(\frac{\partial T_{11}}{\partial x} + \frac{\partial T_{12}}{\partial y}\right) \end{aligned}\right\} \tag{18}$$

and therefore

$$\frac{\partial T_{11}}{\partial x} + \frac{\partial T_{12}}{\partial y} = 0 \qquad \frac{\partial T_{12}}{\partial x} + \frac{\partial T_{22}}{\partial y} = 0 \tag{19}$$

For $LN - M^2$ vanishes on the developable surface. Consequently we can conclude the approximate existence of the stress function for the buckled state of the circular cylindrical shells.

In consequence, we can put

$$T_{11} = Et\chi_{yy} \qquad T_{12} = -Et\chi_{xy} \qquad T_{22} = Et\chi_{xx} \tag{20}$$

using the stress function χ. The compatibility equation can be written as

$$V^4\chi = -\left(LN - M^2\right) \tag{21}$$

neglecting higher order infinitesimals. The deflection w must be chosen so as to minimize the right-hand side of equation (21). If we take equation (13) which could nearly, though not completely, satisfy this condition we have, according to equation (21),

$$\chi = -\frac{\lambda^2}{\left(\lambda^2 + \mu^2\right)^2}\left(2\mu^2 f_1 f_2 - f_1\right)\cos\lambda x \cos\mu y - \frac{1}{16}\left(\frac{1}{2}\frac{\mu^2}{\lambda^2}f_1^2 - \frac{2}{\lambda^2}f_2\right)\cos 2\lambda x - \frac{1}{32}\frac{\lambda^2}{\mu^2}f_1^2\cos\mu y - \frac{\lambda^2\mu^2 f_1 f_2}{\left(\lambda^2 + 9\mu^2\right)^2}\cos\lambda x\cos 3\mu y - \frac{\lambda^2\mu^2 f_1 f_2}{\left(9\lambda^2 + \mu^2\right)^2}\cos 3\lambda x\cos\mu y - \frac{1}{4}\frac{\lambda^2\mu^2}{\left(\lambda^2 + \mu^2\right)^2}f_2^2\cos 2\lambda x\cos 2\mu y - \frac{1}{2}\frac{\sigma}{E}y^2 \tag{22}$$

where σ is positive in compression. Obtaining T_{11}, T_{12}, T_{22}, from equation (20), and then the strain of the middle surface e_{11}, e_{12}, e_{22}, we have

$$\left.\begin{aligned} u_x &= -\frac{\sigma}{E} - \frac{\lambda^2}{8} f_1^2 - \frac{\lambda^2}{4} f_2^2 \\ v_y &= \nu\frac{\sigma}{E} - \frac{\mu^2}{8} f_1^2 - \frac{\mu^2}{4} f_2^2 + f_o \end{aligned}\right\} \tag{23}$$

according to the relations

$$e_{11} = u_x + \frac{1}{2} w_x^2 \qquad e_{22} = v_y - w + \frac{1}{2} w_y^2$$

and neglecting the periodic terms. If we put

$$f_1 = \frac{g_1}{n^2} \qquad f_2 = \frac{g_2}{n^2} \tag{24}$$

by means of equation (3) or (5), g_1 and g_2 may be considered to be approximately constant for the post-buckling surface. The concrete idea for the mechanism of buckling deformation will be obtainable later by introducing these parameters. By equation (5)

$$k = \frac{\lambda}{\mu} = \frac{\lambda}{\eta} \tag{25}$$

and therefore the axial shortening of the cylinder per unit axial length is obtained from equation (23) as

$$e = q + \frac{k^2}{\eta}\left(\frac{1}{8} g_1^2 + \frac{1}{4} g_2^2\right) \tag{26}$$

where

$$q = \frac{\sigma}{E\sqrt{\alpha}} \qquad e = \frac{\sigma}{E} \qquad \eta = n^2\sqrt{\alpha} \tag{27}$$

$$\alpha = \frac{t^2}{12\left(1 - \nu^2\right)a^2} \tag{28}$$

And from the condition $v_y = 0$, we obtain

$$f_o = -\nu \frac{\sigma}{E} + \frac{1}{n^2}\left(\frac{1}{8} g_1^2 + \frac{1}{4} g_2^2\right) \tag{29}$$

Equation (26) shows that the total axial shortening of the cylinder consists of two parts, one of which is the elastic compressive strain

$$e_1 = q \tag{30}$$

caused by the mean compressive stress σ, when the shell is assumed not buckled, and the other is the shortening from the change of the geometrical shape of the surface

$$e_2 = \frac{k^2}{\eta}\left(\frac{1}{8} g_1^2 + \frac{1}{4} g_2^2\right) \tag{31}$$

when the shell is assumed not to be subjected to the compressive stress. Similarly, equation (29) shows that the same circumstances are also satisfied for the mean radial displacement f_o. The fact that equation (31) has the same form as equation (7) will be considered to be the consequence that the buckled surface is similar to the concave polyhedron mentioned previously (fig. 3(a)). The discrepancy in the value of the coefficient $\frac{1}{8} g_1^2 + \frac{1}{4} g_2^2$ from that of $\Pi^2/8$ will be a measure of the deviation of the surface from the completely developable surface.

Denoting the total elastic energy, the extensional, and bending energy by W, W_e and W_b, respectively, and putting

$$\left.\begin{aligned} W &= 2\pi aL \frac{1}{2} Et\alpha\Pi \\ W_e &= 2\pi aL \frac{1}{2} Et\alpha\Pi_e \\ W_b &= 2\pi aL \frac{1}{2} Et\alpha\Pi_b \end{aligned}\right\} \tag{32}$$

L being the length of the cylinder, E the Young's modulus, we have

$$\Pi = \Pi_e + \Pi_b \tag{33}$$

where, by the use of equations (13) and (22),

$$\left.\begin{aligned} \Pi &= \frac{Q}{n^4\alpha} + \left(\frac{\sigma}{E\sqrt{\alpha}}\right)^2 = \frac{1}{\eta^2}\,Q + q^2 \\ \Pi &= Gg_1^{\,2} + Hg_2^{\,2} \end{aligned}\right\} \tag{34}$$

and

$$Q = Ag_1^{\,4} + Bg_1^{\,2}g_2^{\,2} + Cg_2^{\,4} - Dg_1^{\,2}g_2 + Cg_1^{\,2} + Fg_2^{\,2} \tag{35}$$

$$\left.\begin{aligned} A &= \frac{k^4 + 1}{128} \\ B &= k^4\left[\frac{1}{(k^2+1)^2} + \frac{1}{4(9k^2+1)^2} + \frac{1}{4(k^2+9)^2}\right] \\ C &= \frac{k^4}{4(k^2+1)^2} \qquad D = \frac{k^4}{(k^2+1)^2} + \frac{1}{16} \\ F &= \frac{1}{8} \qquad G = \frac{(k^2+1)^2}{4} \qquad H = 2\left(k^4+1\right) \end{aligned}\right\} \tag{36}$$

The extensional energy Π_e consists of the elastic energy q^2 due to the mean stress q and the energy $\frac{1}{\eta^2}Q$ due to the deviation from the mean. The bending energy Π_b does not depend on the circumferential wave number n. The cylindrical shell is distinguished from the flat plate by the fact that the negative term $-Dg_1^{\,2}g_2$ exists in the expression Q, and in consequence of this, Q can diminish to any extent by increasing the number of terms, provided that the value of g_{ij} is chosen appropriately. Contrary to Π_e, the bending energy Π_b increases with the number of terms of the series representing w. Consequently, even for the finite deformation after buckling, the extensional and the bending energy have the same order of magnitude, and this also proves that the deformation is almost inextensional from the energy viewpoint.

Since the buckling load of circular cylindrical shells is to be determined from the energy level before and after buckling, the loading condition must be prescribed. We can consider constant end displacement, constant end load such as by dead weight, or other intermediate states. Among these conditions, the fundamental case of constant end displacement will be treated first. In this case, the axial shortening e must be considered as the independent variable. Therefore, from equation (26), the first equation of (34) becomes

$$\Pi_e = \frac{1}{\eta^2} Q' + e^2 - 2e \frac{k^2}{\eta} \left(\frac{1}{8} g_1^2 + \frac{1}{4} g_2^2 \right) \tag{37}$$

where

$$Q = A' g_1^4 + B' g_1^2 g_2^2 + C' g_2^4 - D g_1^2 g_2 + C g_1^2 + F g_2^2 \tag{38}$$

$$\left.\begin{aligned} A' &= A + \frac{k^4}{64} \\ B' &= B + \frac{k^4}{64} \\ C' &= C + \frac{k^4}{64} \end{aligned}\right\} \tag{39}$$

Since the work of the external force is zero under the condition e = const., we have the equilibrium condition

$$\delta W = 0$$

or, assuming the dimensions of the shell to be given,

$$\frac{\partial \Pi}{\partial g_1} = 0 \qquad \frac{\partial \Pi}{\partial g_2} = 0 \tag{41}$$

under the condition that e, $\eta(n)$ and k are constant, because Π is considered to be

$$\Pi = \Pi(e, \eta(n), k, g_1, g_2) \tag{42}$$

From equation (41) we obtain

$$\left.\begin{aligned} \frac{1}{\eta^2}\left[4A'g_1^2 + 2B'g_1^2\rho^2 - 2Dg_1\rho + 2C\right] + 2G - \frac{1}{2}e\frac{k^2}{\eta} = 0 \\ \frac{1}{\eta^2}\left[2B'g_1^2\rho + 4C'g_1^2\rho^3 - Dg_1 + 2F\rho\right] + 2H\rho - e\frac{k^2}{\eta}\rho = 0 \end{aligned}\right\} \quad (43)$$

$$g_2/g_1 = \rho$$

Eliminating e from equation (43), we have an equation of the third order with respect to ρ, namely,

$$4(B' - C')g_1^2\rho^3 - 4Dg_1\rho^2 +$$

$$\left[(8A' - 2B')g_1^2 + 4C - 2F + \eta^2(4G - 2H)\right]\rho + Dg_1 = 0 \quad (44)$$

Substituting the value of ρ, obtained from equation (44) with parameters k, η and g_1, into the first equation of (43), we obtain e, and then q from equation (26). The relationship between q and g_1 is shown in figure 4 for each case of $k = 0.2$, 0.6, and 1.0. Though the value of g_1 for the post-buckling equilibrium state is not determined from these curves, the fact that all curves lie within a definite range of g_1 and show a similar shape, indicates the reasonability of the assumption (24).

The relation between q and e is shown in figure 5 with k and η as parameters. The minimum value of q, corresponding to the branch points of the curves exhibiting the post-buckling state, is the critical load by the classical theory

$$q = 2$$

as is well known.

It is important that the curves in figure 5 reveal the condition Π = min. (only under the restriction k), η = const. but do not give the minimum condition of $\Pi\left(e, \eta, k, g_1, g_2\right)$ with respect to each of its independent variables. Therefore, the inference that the smallest

value of q in figure 5 will be realized after buckling, is erroneous. In other words, the fact that q is negative and has a large absolute value for small values of k means that the geometrical shortening (31) is greater than the total shortening e, and therefore the extensional energy Π_e is increased under such conditions, and Π does not become minimum.

As was stated above, for the determination of the post-buckling state, it is necessary to determine the values of e, η, k, g_1, and g_2, and hence of q, corresponding to the minimum value of the hypersurface (e, η, k, g_1, g_2) with regard to the variables e, η, k, g_1 and g_2. For this purpose, we need to inquire into the minimum value, with respect to η and k, of the minimum of Π in a section η, $k = \text{const}$. Figure 6 shows the value of the total strain energy Π calculated from figures 4 and 5, taking k and η as parameters. Hence, this calculation gives the minimum of Π for each section. Each curve in figure 6 has the form as shown in figure 7(a). For $e < e^*$ in the figure, buckling is impossible, but for $e^* \leqq e < e_o$, it is not impossible if some energy is supplied from the exterior. It is for $e \geqq e_o$ that buckling takes place in general, but for this a certain amount of energy barrier must be jumped over. At $e = e_1 > e_o$, for example, the energy barrier corresponding to CC' must be jumped over in order that the equilibrium position shifts from C to C" by buckling. This process can be illustrated as in figures 7(b) and (c) with g_1 or q as the independent variable. As the buckling load corresponding to e_1 increases, the energy barrier to be jumped over decreases, and the energy difference before and after buckling increases.

From figure 6, it is shown that the value of g_1 and g_2 corresponding to e_o is almost constant, independent of k and η; this is worth noting as indicating that the starting assumption (24) is reasonable.

Denoting the minima of e_o with respect to η for each value of k in figure 6 by $e_{o,m}$, and the values of Π at S and S' and that of η at S (refer to fig. 7) corresponding to $e_{o,m}$ by $\Pi_{o,m}$, $\Pi_{o,m}$, and η_m, respectively, we can obtain the manner in which these quantities change against k (fig. 8). The value of $\Pi_{o,m}$ seems to show a minimum $\Pi_{o,m,m}$ near $k = 0.2$, and the corresponding value of $e_{o,m}$ is about 1.3 and that of η_m 0.02. Therefore the buckling load in this

case is $q = 1.3$, while the load after buckling is estimated roughly as $q = 0.9$. The energy barrier to be jumped over is approximately $\Pi_b = 0.14$, which is equal to about one tenth of the energy just before buckling. Generally, buckling occurs for $q \geq 1.3$, since the value $q = 1.3$ corresponding to $\Pi_{o,m,m}$ is the minimum buckling load. The greater the buckling load, the smaller the energy barrier, i.e., the more likely buckling will occur, while the greater the energy difference before and after buckling, i.e., the greater the sound or vibration is generated with buckling. The problem, at what load over the minimum buckling load the actual buckling will occur, is to be decided by the initial deformation of the shell and the conditions of the experiments. With a constant value of e greater than 1.3, the value of k and consequently of η, corresponding to the minimum of the energy is somewhat greater than that for the case $e = 1.3$. Therefore, as the actual buckling load increases over the minimum buckling load, the lobes have a tendency to become short and thick in the axial direction, and the circumferential wave number increases. The energy curve for any constant e is very flat in the neighborhood of its minimum, hence the post-buckling state cannot be determined sharply, but will be scattered over a certain range. At any rate, the lobes in the case of the general buckling are found to be very slender in the axial direction.

Though the general buckling was not realized in experiments with comparatively long cylinders, it will be realized if a cylinder of a particular length, corresponding to 1.5 times of the wave length, is used.

LOCAL BUCKLING

According to the experimental results, actual buckling is local, consequently there exist two parts, one of which is buckled and the other unbuckled. The occurrence of local buckling is explained qualitatively from the following energy consideration. If local buckling were assumed to take place at the minimum buckling load of general buckling, the load supported by the buckled part would decrease abruptly; and in consequence of the fall of the load, the elastic energy of the unbuckled part will decrease more than the energy increase of the buckled part. Hence the total elastic energy would become smaller after buckling under fixed end displacement. This means that the minimum buckling load in the case of local buckling will be found below the general buckling load. The occurrence of local buckling, on the other hand, is inferred from the genetic viewpoint that the stress-strain relation after buckling (fig. 5) is such that the velocity of propagation of the buckling deformation is nearly zero.

In this paragraph we shall consider this problem from the energy standpoint on the basis of the results on general buckling. Dividing the entire cylinder into the buckled and the unbuckled parts and writing

	Buckled part	Unbuckled part	Entire cylinder
Length	L_1	L_2	L
Mean compressive stress	σ_1	σ_2	σ
Compression	ϵ_1'	ϵ_2'	ϵ'
Elastic energy	W_1'	W_2'	W

we have

$$L = L_1 + L_2 \tag{45}$$

$$q_1 = q_2 = q = Ee_1' \tag{46}$$

$$W' = W_1' + W_2' \tag{47}$$

$$Le' = L_1 e_1' + L_2 e_2' \tag{48}$$

where

$$\left.\begin{aligned} e' &= \frac{\epsilon'}{\sqrt{\alpha}} & e_1' &= \frac{\epsilon_1'}{\sqrt{\alpha}} & e_2' &= \frac{\epsilon_2'}{\sqrt{\alpha}} \\ q &= \frac{\sigma}{E\sqrt{\alpha}} & q_1 &= \frac{\sigma_1}{E\sqrt{\alpha}} & q_2 &= \frac{\sigma_2}{E\sqrt{\alpha}} \end{aligned}\right\} \tag{49}$$

Eliminating e_1' and e_2' from equations (46), (26), and (48), we obtain

$$e' = q + \frac{L_2}{L}\frac{k^2}{\eta}\left(\frac{1}{8}g_1^2 + \frac{1}{4}g_2^2\right) \tag{50}$$

Equation (50) shows that the total axial shortening depends on the length L_2 of the buckled part. As we can put

$$L_2 = 1.5(2l_x) \tag{51}$$

from the experimental results, we have

$$L_2 = \frac{3\pi a}{nk} \tag{52}$$

from equations (5) and (12). Therefore equation (50) is written as

$$e' = q + \frac{3\pi a}{Lnk}\frac{k^2}{\eta}\left(\frac{1}{8}g_1^2 + \frac{1}{4}g_2^2\right) \tag{53}$$

The second term of the right-hand side of equation (53) represents the geometrical shortening due to local buckling.

The total elastic energy is the sum of the elastic energy of the unbuckled part.

$$W_1' = 2\pi atL_1\frac{1}{2}E\epsilon_1'^2 = 2\pi aL_1\frac{Et}{2}\alpha q^2 \tag{54}$$

and that of the buckled part

$$W_2' = \frac{L_2}{L}W \tag{55}$$

where W is given by equations (32) and (34). Hence, putting

$$\left.\begin{aligned} W' &= 2\pi aL\frac{1}{2}Et\alpha\Pi \\ W_1' &= 2\pi aL\frac{1}{2}Et\alpha\Pi' \\ W_2' &= 2\pi aL\frac{1}{2}Et\alpha\Pi_2' \end{aligned}\right\} \tag{56}$$

it follows

$$\left.\begin{aligned} \Pi_1' &= \frac{L_1}{L}q^2 \\ \Pi_2' &= \frac{L_2}{L}\left[\frac{1}{\eta^2}Q + q^2 + \left(Gg_1^2 + Hg_2^2\right)\right] \end{aligned}\right\} \tag{57}$$

or by means of equation (52)

$$\Pi' = \Pi_1' + \Pi_2' = \frac{3\pi a}{Lnk}\left[\frac{1}{\eta^2}Q'' + \left(Gg_1^2 + Hg_2^2\right)\right] + q^2 \tag{58}$$

Considering e' to be the independent variable, equation (58) is written as

$$\Pi' = \frac{3\pi a}{Lnk}\left[\frac{1}{\eta^2}Q'' + \left(Gg_1^2 + Hg_2^2\right)\right] + e'^2 - 2e'\frac{3\pi a}{Lnk}\frac{k^2}{\eta}\left(\frac{1}{8}g_1^2 + \frac{1}{4}g_2^2\right) \tag{59}$$

by equation (53), where

$$Q'' = A''g_1^4 + B''g_1^2g_2^2 + C''g_2^4 - Dg_1^2g_2 + Cg_1^2 + Fg_2^2 \tag{60}$$

$$\left.\begin{aligned} A'' &= A + \frac{3\pi a}{Lnk}\frac{k^4}{64} \\ B'' &= B + \frac{3\pi a}{Lnk}\frac{k^4}{64} \\ C'' &= C + \frac{3\pi a}{Lnk}\frac{k^4}{64} \end{aligned}\right\} \tag{61}$$

The minimum condition for W', or $\frac{\partial \Pi'}{\partial g_1} = 0$ and $\frac{\partial \Pi'}{\partial g_2} = 0$ under the condition e', η, k = const. is given by

$$\left.\begin{aligned} &\frac{1}{\eta^2}\left[4A''g_1^2 + 2B''g_1^2\rho^2 - 2Dg_1\rho + 2C\right] + 2G - \frac{e'}{2}\frac{k^2}{\eta} = 0 \\ &\frac{1}{\eta^2}\left[2B''g_1^2\rho + 4C''g_1^2\rho^3 - Dg_1 + 2F\rho\right] + 2H\rho - e'\frac{k^2}{\eta}\rho = 0 \end{aligned}\right\} \tag{62}$$

Eliminating e' from equation (62), we have

$$4(B'' - C')g_1^2\rho^3 - 4Dg_1\rho^2 + \left[(8A'' - 2B'')g_1^2 + 4C - 2F + \eta^2(4G - 2H)\right]\rho + Dg_1 = 0 \tag{63}$$

which is equivalent to equation (44), as the relation

$$\left.\begin{aligned} B'' - C'' &= B' - C' = B - C \\ 8A'' - 2B'' &= 8A' - 2B' = 8A - 2B \end{aligned}\right\} \tag{64}$$

is satisfied by means of equations (61) and (39). Consequently, we can use the same results regarding g_1, ρ, and η as were calculated in the case of general buckling. Comparing e', obtained from the first equation of (62) by means of calculated results, with e derived from the first equation of (43), we have

$$e' = e + \left(\frac{3\pi a}{Lnk} - 1\right) \frac{k^2}{\eta} \left(\frac{1}{8} g_1^2 + \frac{1}{4} g_2^2\right) \tag{65}$$

This equation reduces to equation (53) by virtue of equation (26), so that the value of q in the case of local buckling is the same as that of q in the case of general buckling. Hence, we need not carry out the calculation for the local buckling under the condition $e' = \text{const.}$ all over again, but only calculate e' and Π', which satisfy the minimum condition of energy with respect to g_1 and g_2, by equations (53) and (58), respectively, using the results calculated for the case of general buckling. Local buckling differs from the case of general buckling in that it depends on the dimensions a, L, t and the Poisson's ratio ν of the circular cylinder, and therefore on the value of n.

Using the values $a = 111$ mm, $L = 460$ mm, $t = 0.4$ mm, and $\nu = 0.4$ for the shells used in the experiments, the $e' \sim q$ and the $e' \sim \Pi'$ relations are calculated as shown in figure 9 and figure 10, respectively. As in the case of general buckling, we can define for local buckling e_o', Π_o', $\Pi_{\bar{o}}'$ and $e'_{o,m}$, $\Pi'_{o,m}$, $\Pi'_{\bar{o},m}$, η_m corresponding to the minimum of Π_o' with fixed k. The manner in which these quantities change against k is shown in figure 11. The minimum $e'_{o,m,m}$ or $\Pi'_{o,m,m}$ of $e'_{o,m}$ or $\Pi'_{o,m}$ exists near $k = 0.7$, and $e'_{o,m,m} = 1.04$, and the corresponding value of η is approximately 0.10 (or $n = 9.40$). The post-buckling load for $e' = e'_{o,m,m} = 1.04$, $k = 0.7$ and $\eta = 0.10$ is obtained as about $q = 0.7$, and the energy barrier $\Pi'_{\bar{o},m,m} - \Pi'_{o,m,m}$ about 0.07. The post-buckling state when buckling occurs at any load above the minimum buckling load $q = e'_{o,m,m} = 1.04$, will be determined

by the minimum energy condition at e' corresponding to the buckling load q. This state, however, does not differ greatly from that of minimum energy represented in figure 11.

Comparing figure 11 with figure 8, it is seen that the minimum energy $\Pi'_{o,m,m}$ for the local buckling is much smaller than the minimum energy $\Pi_{o,m,m}$ for the general buckling, and this means that the local buckling is more liable to occur. As the $\Pi'_{o,m}$ curve shows a sharper minimum than that for $\Pi_{o,m}$, the post buckling state for local buckling will not be scattered as widely as in general buckling.

The above calculation was carried out under the assumption that the end shortening is constant before and after buckling. Hence the results may be compared with experiment 1 (fig. 1) performed with a spring of large rigidity (table 1). The agreement of the value of k is good, but that of the buckling load, the load after buckling and the circumferential wave number, is not very good.

LOCAL BUCKLING WITH ELASTIC LOAD EQUIPMENT

Actually, it is impossible to realize the condition e or $e' = \text{const.}$ in buckling by usual testing machines. The absorption of energy by the testing machine is inevitable due to the finite rigidity of the structural material of the testing machine, even when springs or oil pressure is not used. The absorbed energy increases with the decrease of the rigidity of the machine, and it is natural that the interchange of energy between the machine and test specimens have some effect on the buckling phenomenon. In the present paragraph, a case in which the rigidities of both the loading equipment and the testing machine are replaced by a spring, will be analyzed and compared with the experimental result.

It is assumed that a shell undergoes local buckling as in the preceding paragraph. Denoting the shortening of the cylinder per unit length by $\epsilon'\left(e' = \epsilon'/\sqrt{\alpha}\right)$ as before, the length, the unit compression and the rigidity of the spring by L_s, $\epsilon_s\left(e_s = \epsilon_s/\sqrt{\alpha}\right)$ and E_s, respectively, and the length and the unit compression of the total system containing both the cylinder and the spring by L_t and $\epsilon_t\left(e_t = \epsilon_t\sqrt{\alpha}\right)$, respectively, we have

$$L_t = L + L_s \tag{66}$$

$$L_t e_t = Le' + L_s e_s \tag{67}$$

$$e_s = 2\pi \text{ at } q\frac{E}{E_s} \tag{68}$$

Substituting equations (53) and (68) into equation (67), the shortening of the total system is given by

$$\frac{L_t}{L} e_t = \left(1 + \frac{L_s}{L} \frac{2\pi atE}{E_s}\right) q + \frac{3\pi a}{Lnk} \frac{k^2}{\eta} \left(\frac{1}{8} g_1^2 + \frac{1}{4} g_2^2\right) \tag{69}$$

As the elastic energy of the spring is given by

$$W_s = \frac{1}{2} L_s E_s \epsilon_s^2$$

or

$$\left.\begin{aligned} W_s &= 2\pi aL \frac{1}{2} Et\alpha \Pi_s \\ \Pi_s &= \frac{L_s}{L} \frac{2\pi atE}{E_s} q^2 \end{aligned}\right\} \tag{70}$$

the elastic energy of the total system is given by

$$\left.\begin{aligned} W'' &= 2\pi aL \frac{1}{2} Et\alpha \Pi'' \\ \Pi'' &= \frac{3\pi a}{Lnk} \left[\frac{1}{\eta^2} Q + \left(Gg_1^2 + Hg_2^2\right)\right] + \left(1 + \frac{L_s}{L} \frac{2\pi atE}{E_s}\right) q^2 \end{aligned}\right\} \tag{71}$$

using equations (56) and (58). The energy carried by the spring is proportional to L_s/L and E/E_s.

The buckling in this case is to be considered with e_t as an independent variable, which was e' in the case of local buckling. Substituting, therefore, q of equation (69) into equation (71), we obtain

$$\Pi'' = \frac{3\pi a}{Lnk} \left[\frac{1}{\eta^2} Q''' + \left(Gg_1^2 + Hg_2^2\right)\right] + \frac{1}{1 + (L_s/L)(2\pi atE/E_s)} \left[\left(\frac{L_t}{L} e_t\right)^2 - 2 \frac{L_t}{L} e_t \frac{3\pi a}{Lnk} \frac{k^2}{\eta} \left(\frac{1}{8} g_1^2 + \frac{1}{4} g_2^2\right)\right] \tag{72}$$

$$Q''' = A'''g_1^4 + B'''g_1^2g_2^2 + C'''g_2^4 - Dg_1^2g_2 + Cg_1^2 + Fg_2^2 \quad (73)$$

$$\left.\begin{aligned} A''' &= A + \frac{3\pi a/(Lnk)}{1 + \left(L_s/L\right)\left(2\pi atE/E_s\right)} \frac{k^4}{64} \\ B''' &= B + \frac{3\pi a/(Lnk)}{1 + \left(L_s/L\right)\left(2\pi atE/E_s\right)} \frac{k^4}{64} \\ C''' &= C + \frac{3\pi a/(Lnk)}{1 + \left(L_s/L\right)\left(2\pi atE/E_s\right)} \frac{k^4}{64} \end{aligned}\right\} \quad (74)$$

The equilibrium condition under constant n and k is given by

$$\frac{\partial \Pi''}{\partial g_1} = 0 \qquad \frac{\partial \Pi''}{\partial g_2} = 0$$

or

$$\left.\begin{aligned} &\frac{1}{\eta^2}\left[4A'''g_1^2 + 2B'''g_1^2\rho - 2Dg_1\rho + 2C\right] - \frac{1}{2}\frac{\left(L_t/L\right)e_t}{1 + \frac{L_s}{L}\frac{2\pi atE}{E_s}}\frac{k^2}{\eta} + 2G = 0 \\ &\frac{1}{\eta^2}\left[2B'''g_1^2\rho + 4C'''g_1^2\rho^3 - Dg_1 + 2F\rho\right] - \frac{\left(L_t/L\right)e_t}{1 + \frac{L_s}{L}\frac{2\pi atE}{E_s}}\frac{k^2}{\eta}\rho + 2H\rho = 0 \end{aligned}\right\} \quad (75)$$

from which, eliminating e_t, the same equation of the third order with respect to ρ as equations (44) and (63) is derived by means of equation (74). Hence, the calculated results of q, η, k, and ρ in the case of general buckling may be used also in this case. It is convenient to use equation (71) instead of equation (72) for the calculation of energy, and equation (69) in place of equation (75) for the calculation of e_t. Figures 12 and 13 show the relations $\Pi'' \sim \left(L_t/L\right)e_t$ and

$\Pi'' \sim e'$, respectively, for a spring with $L_s = 46$ mm, $E_s = 3{,}680$ kg used in experiment 2 and for the same cylindrical shell as in the last paragraph, while figures 14 and 15 show those for a spring with $L_s = 43$ mm, $E_s = 1{,}160$ kg (experiment 3.) The minimum buckling load is given by the value of e' or q corresponding to the minimum $e_{t,o,m,m}$ with respect to k and η of $e_{t,o}$, which is the value of e_t corresponding to the intersecting point of the post-buckling energy curve with the parabolic curve in figures 12 and 14.

As e_t is constant before and after buckling in our experiments, the buckling load and the post-buckling state will be determined by considering these energy charts under the condition $e_t = \text{const}$. For any value of e_t above $e_{t,o,m,m}$ in figures 12 or 14, the corresponding value of Π'' is obtained on the parabola, hence the value of e' or the buckling load q is obtained from figures 13 or 15. The post-buckling state is determined by the following process. The values of k, $\eta(n)$ and Π'' which give the minimum energy for the given e_t are determined from figures 12 or 14, then the corresponding value of e' is determined from figures 13 or 15, and finally, the post-buckling load q corresponding to these values of k, η and e' is determined from figure 9.

The results calculated by the above procedure for the shell and the spring in experiments 2 and 3 are shown in table 1. In comparing with experimental results, the qualitative agreement between the theory and the experiment seems to be satisfactory. The reason that the observed minimum buckling loads in experiments 2 and 3 are not so small compared with those in experiment 1 may be due to the magnitude of the energy barrier. Practically, the supposition that the buckling in experiments 2 and 3 might occur at greater difference of the energy before and after buckling compared with experiment 1, or at energy barrier closer to experiment 1, is confirmed by the fact that the sound on buckling was greater in the former cases than in the latter case. It may be presumed, consequently, that the occurrence of buckling is governed both by the magnitude of the minimum buckling load and the energy barrier.

DEFORMATION AND STRESS DISTRIBUTION

In order to clarify at what part of the buckled shell the compressive load is supported, we calculated the stress distribution (fig. 17) for the deflection w due to equation (13) (fig. 16). According to the result obtained for the post-buckling state $q = 0.7$, $k = 0.7$, and $\eta = 0.10$ $(n = 9.4)$, the compressive load applied to the cylinder is found to be supported by the cross-hatched part.

CONCLUSIONS

The buckled surface of a circular cylindrical shell under axial compression is considered to approximate a particular developable surface, so that the deformation in this case is almost inextensional and finite. The mechanism of buckling of a circular cylindrical shell can be said, in effect, to be a phenomenon of a kind of "Durchschlag."

When the cylinder is loaded by a specified end shortening, the state realized after buckling is determined by the minimum condition of the hypersurface representing the elastic energy with respect to all variables. In consequence, there exists the minimum buckling load which is determined by the equality of the energy before and after buckling and is smaller than the critical load by the classical theory. Actual buckling takes place above this minimum buckling load, by jumping over a certain magnitude of energy barrier, which decreases with the increase of the buckling load. The buckling load will be considered to be governed by both the minimum buckling load and the energy barrier.

From the above viewpoint, local buckling is more likely to occur than general buckling, the minimum buckling load and the energy barrier for the former being smaller than those for the latter. In the case of local buckling, the minimum buckling load decreases as the rigidity of the loading spring decreases. Similarly, the fact that the minimum buckling load for the local buckling is smaller than that for the general buckling is attributable to the spring action of the unbuckled part.

Finally, it will be remarked that scale effects exist for the local buckling as is seen in equations (73) and (75), i.e., that the buckling strength is influenced by the absolute value of the length, radius, and thickness of the cylindrical shell even under the condition of their constant ratios. A paper concerning this effect will be published soon (ref. 7).

The author wishes to express his appreciation to Professor M. Yoshiki for discussions. This research was carried out by the financial aid of the Ministry of Education.

Translated by Y. Yoshimura

Edited by Drs. Y. C. Fung and E. E. Sechler
California Institute of Technology

REFERENCES

1. Robertson, A.: The Strength of Tubular Struts. Proc. Roy. Soc. (London), ser. A, vol 121, 1928, pp. 558-585.

2. Lundquist, Eugene E.: Strength Tests of Thin-Walled Duralumin Cylinders in Compression. NACA Rep. 473, 1933.

3. Donnell, L. H.: A New Theory for the Buckling of Thin Cylinders Under Axial Compression and Bending. A.S.M.E. Trans., vol. 56, no. 11, Nov. 1934, pp. 795-806.

4. Von Karman, Theodore, and Tsien, Hsue-Shen.: The Buckling of Thin Cylindrical Shells Under Axial Compression. Journ. Aero. Sci., vol. 8, no. 8, June 1941, pp. 303-312.

5. Kono, T.: Theoretical Investigation on Elastic Instability of Thin Curved Shells Compressed Axially. Journ. Soc. Aero. Sci. Japan, 8, 1941, p. 178.

6. Yoshimura, Y.: Theory of Thin Shells with Finite Deformation. Rep. Inst. Sci. and Tech., Tokyo Univ., 2, 1948, p. 167; 3, 1949, p. 19.

7. Yoshimura, Y.: Local Buckling of Circular Cylindrical Shells and Scale Effects. Proc. of the 1st Japan National Congress for Appl. Mech., 1951.

TABLE I

			General buckling	Local buckling		
				Loading with constant end displacement	Loading with spring	
				Exp. 1	Exp. 2	Exp. 3
Minimum buckling load (q)		Calculated Observed	1.3	1.04 0.8	0.80 0.76	0.80 0.72
Energy barrier (Π, Π', Π'')			0.14	0.07	0.20	0.10
Post-buckling state	q	Calculated Observed	0.9	0.7 0.4	0.55 0.24	0.70 0.22
	k	Calculated Observed	0.2	0.7 0.64 ~ 0.68	0.75 0.93	0.80 0.95
	$\eta(n)$	Calculated Observed	0.02	0.10 (9.4) 6 ~ 7	0.085 (8.6) 6	0.085 (8.6) 5
	e'	Calculated Observed			1.0 3.2	1.25 4.4

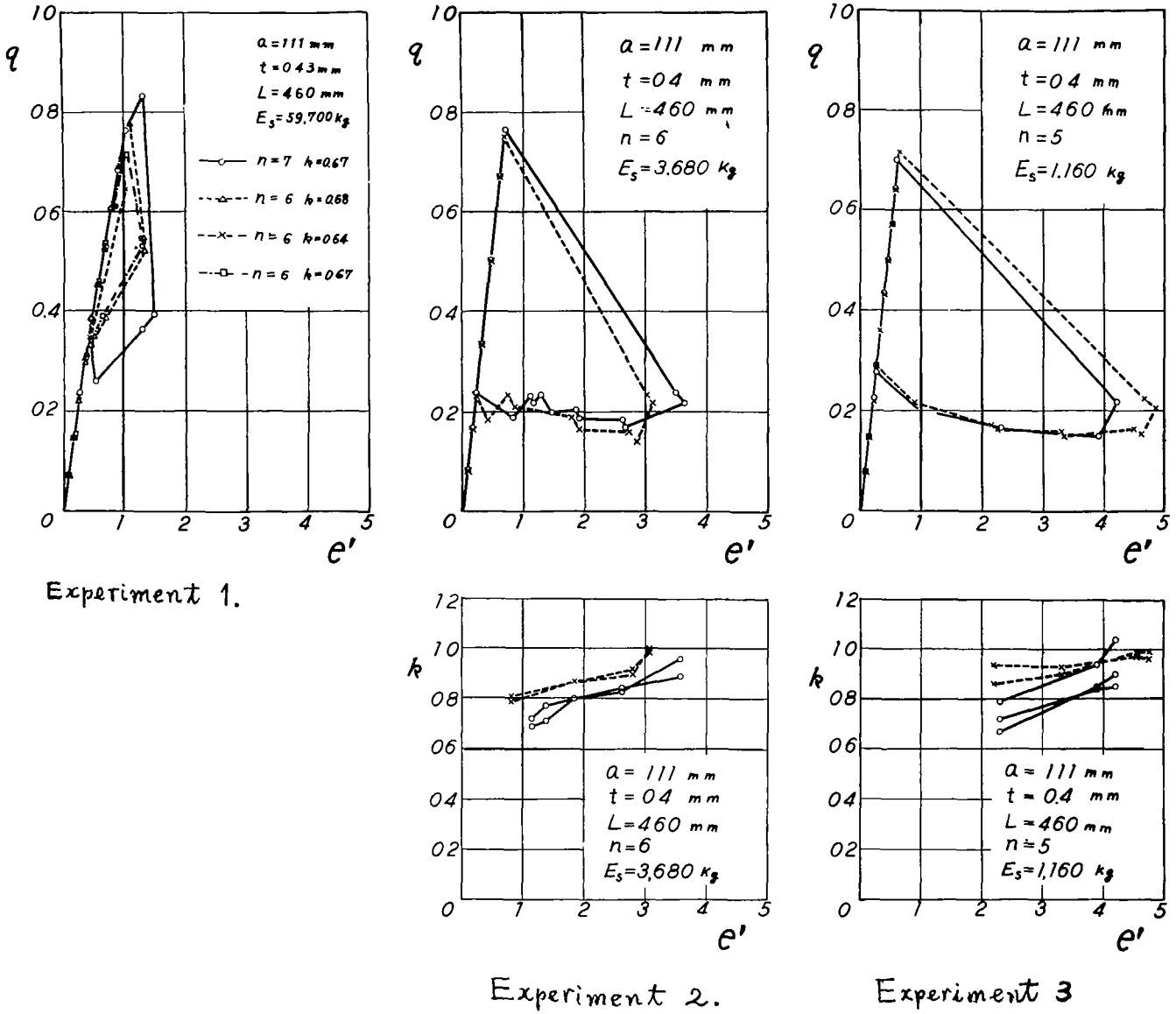

Experiment 1.

Experiment 2.

Experiment 3

Figure 1.- Experimental results of the compressive stress σ and aspect ratio k of the buckling lobes against the unit end shortening ϵ', being $g = \frac{\sigma}{E\sqrt{\alpha}}$, $e' = \frac{\epsilon'}{\sqrt{\alpha}}$, $\alpha = \frac{t^2}{12(1-\nu^2)a^2}$, a = the radius, t = the thickness of the shells.

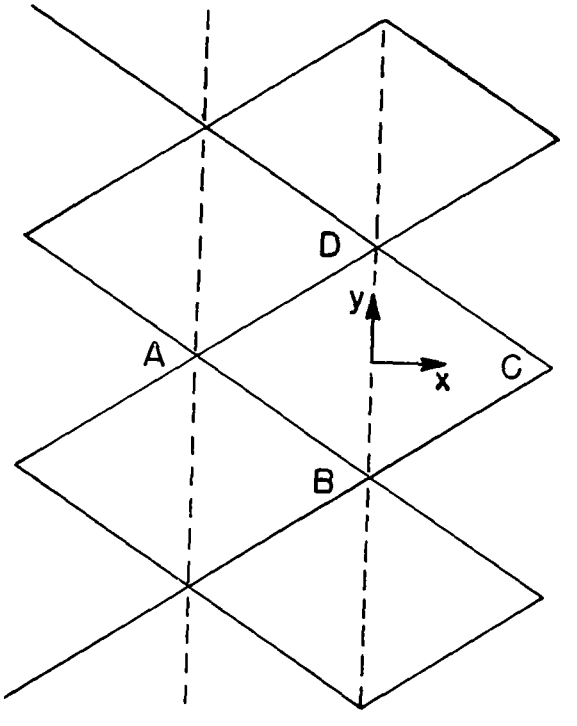

Figure 2.- Developed view of the buckled surface.

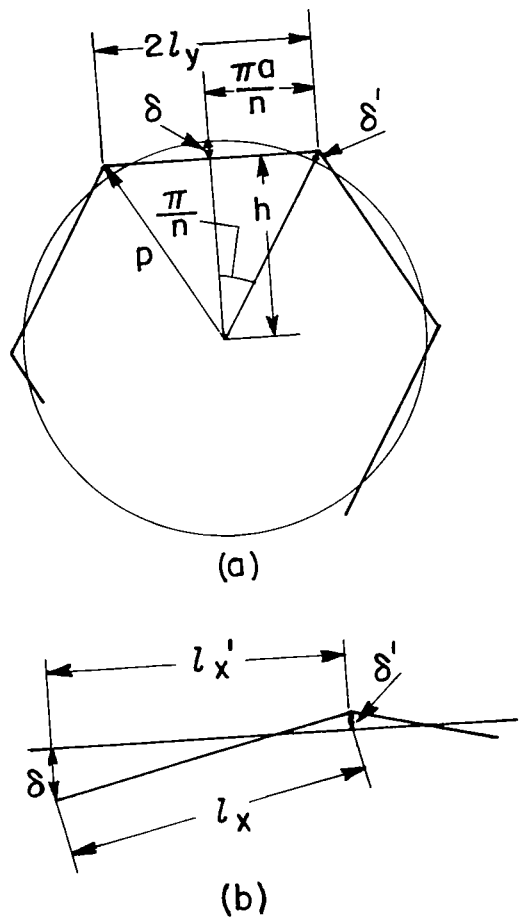

Figure 3.- Cross and longitudinal sections of the buckled surface.

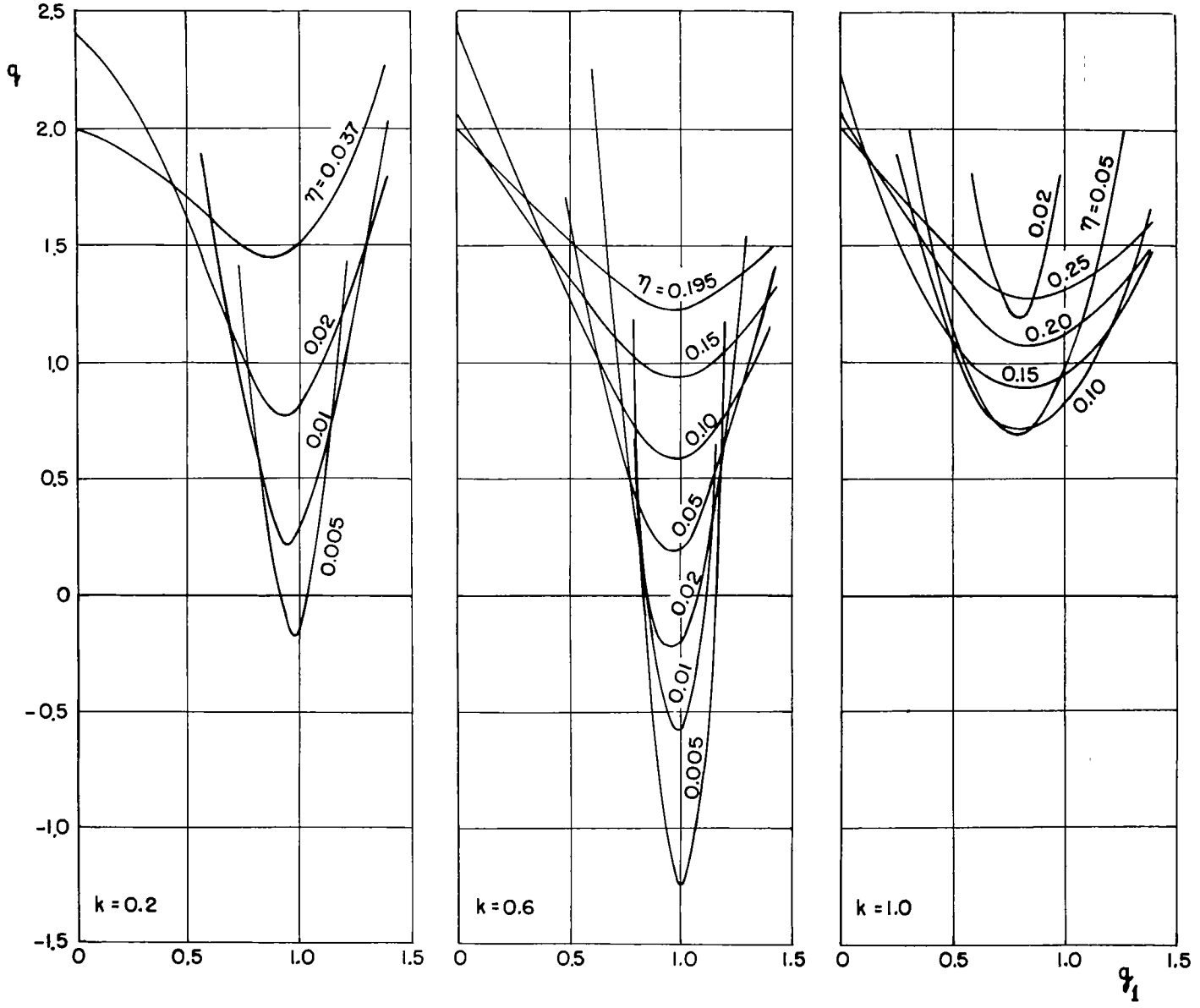

Figure 4.- Relation between the stress q and the deflection g_1 after buckling.

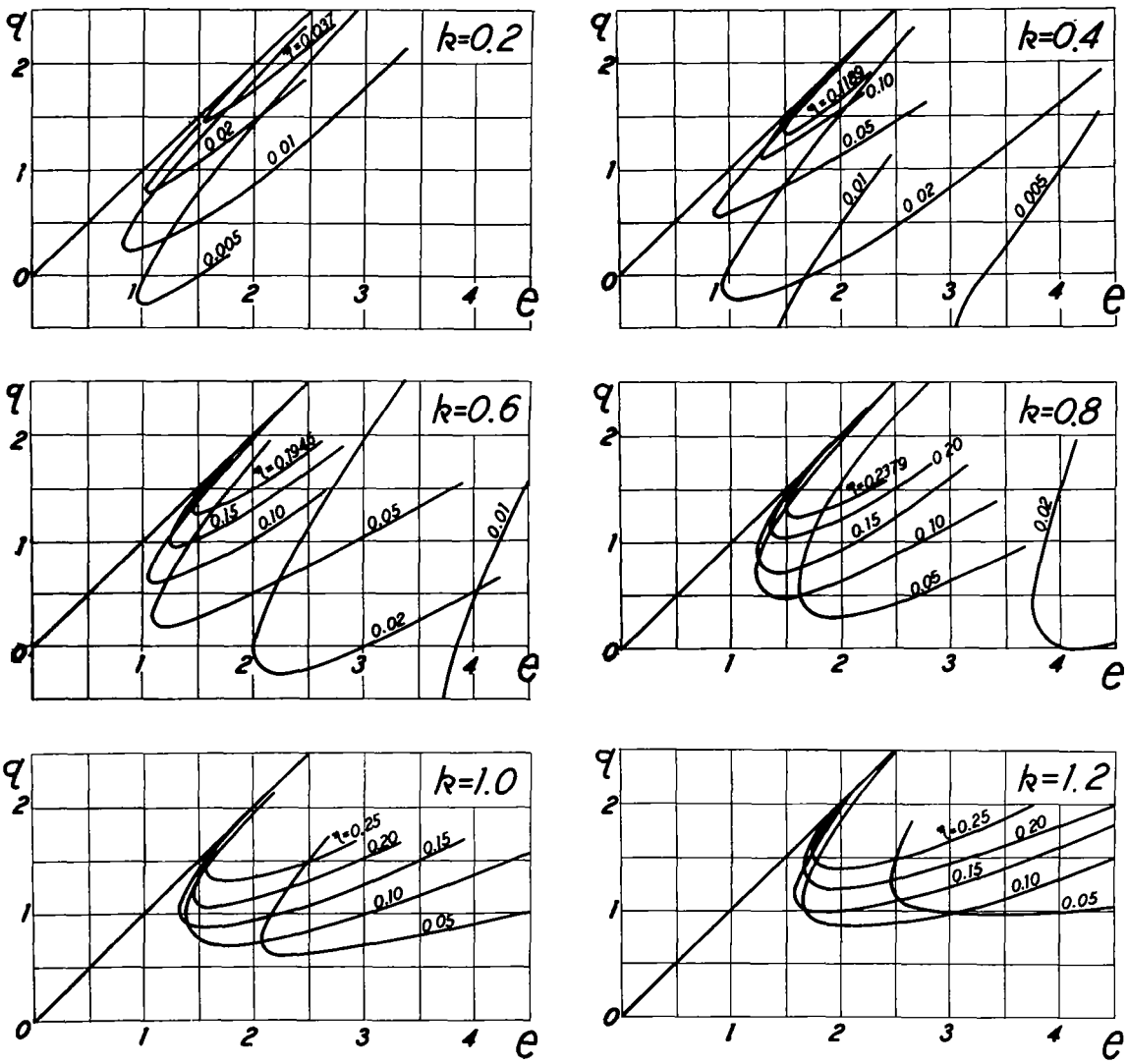

Figure 5.- Relation between the stress q and the unit end shortening e for general buckling.

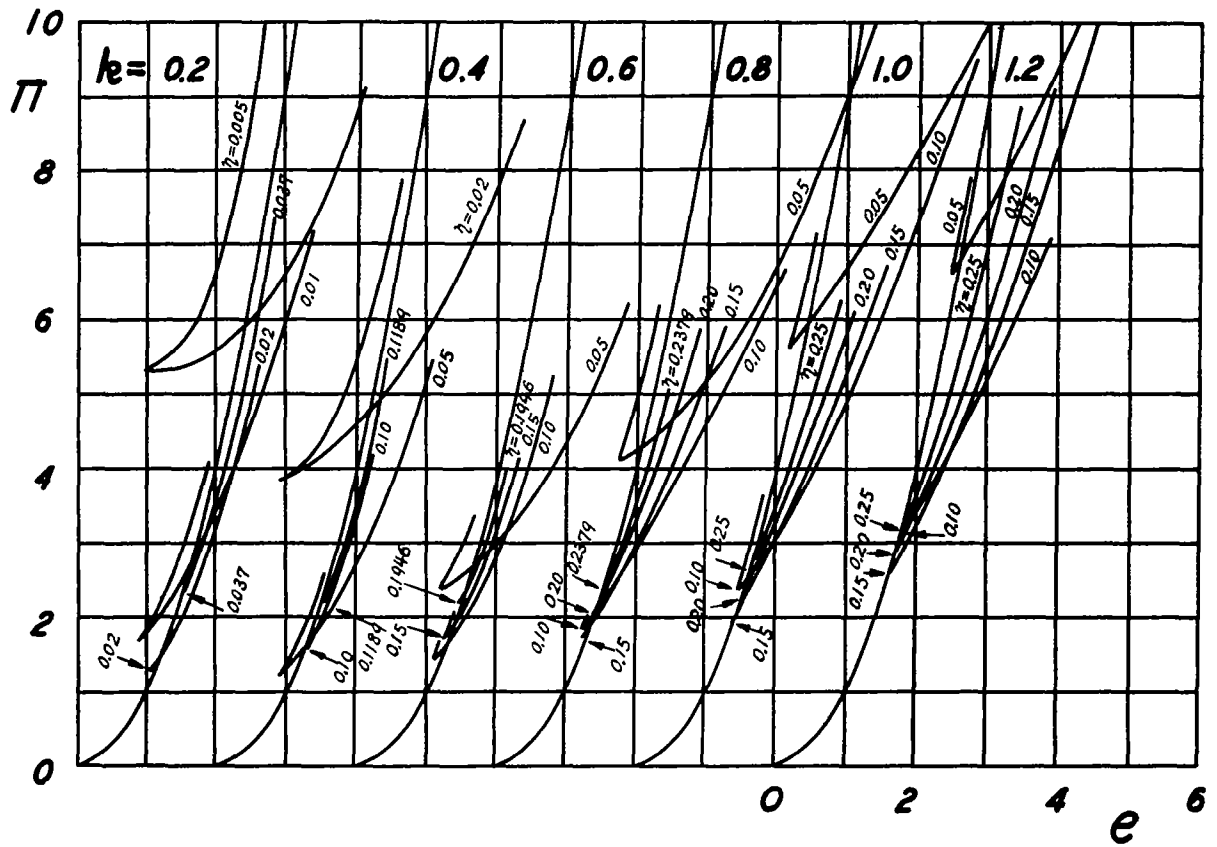

Figure 6.- Relation between the elastic energy Π corresponding to its minimum condition with constant k and η and the unit end shortening e for general buckling.

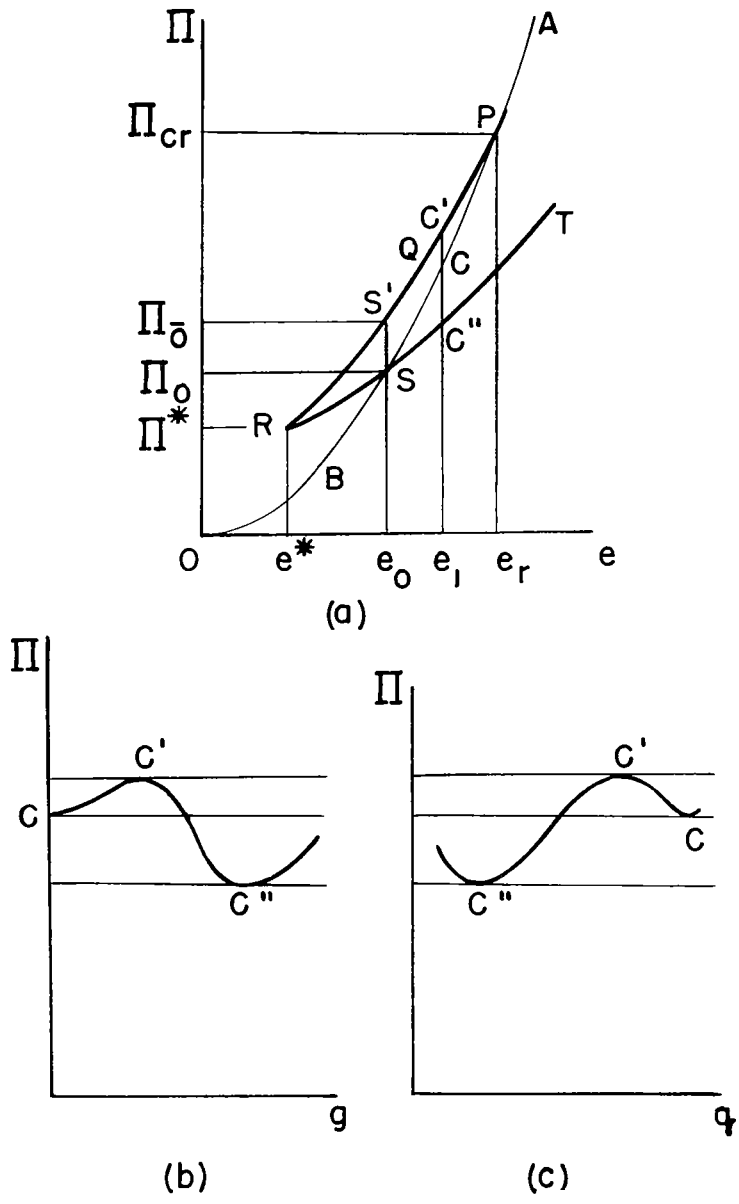

Figure 7.- The energy level before and after buckling and the energy barrier to be jumped over with buckling.

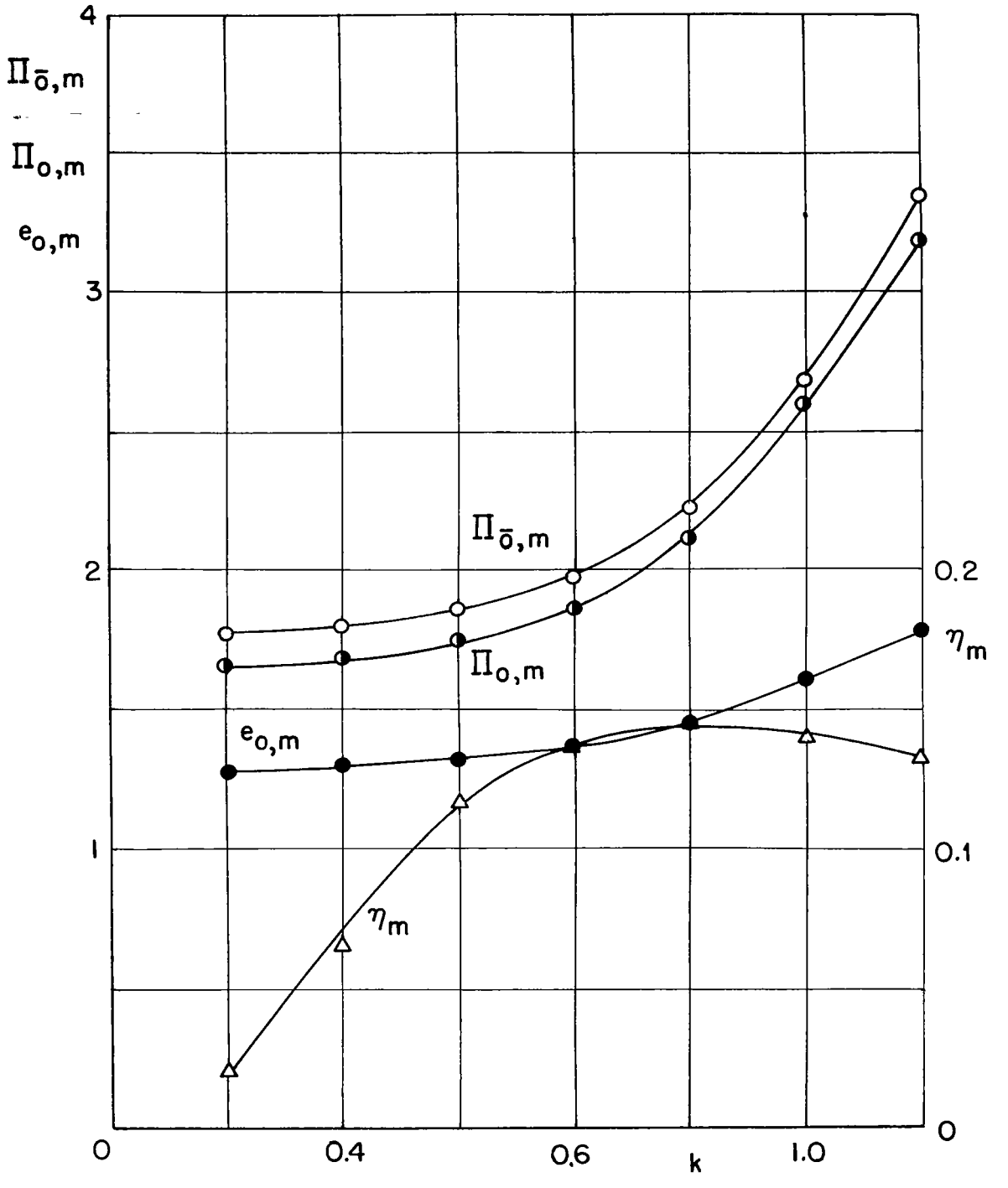

Figure 8.- Relation between the minimum $\Pi_{o,m}$ of the elastic energy, which is equal before and after buckling, with respect to η and the aspect ratio k of the buckling lobes, for general buckling.

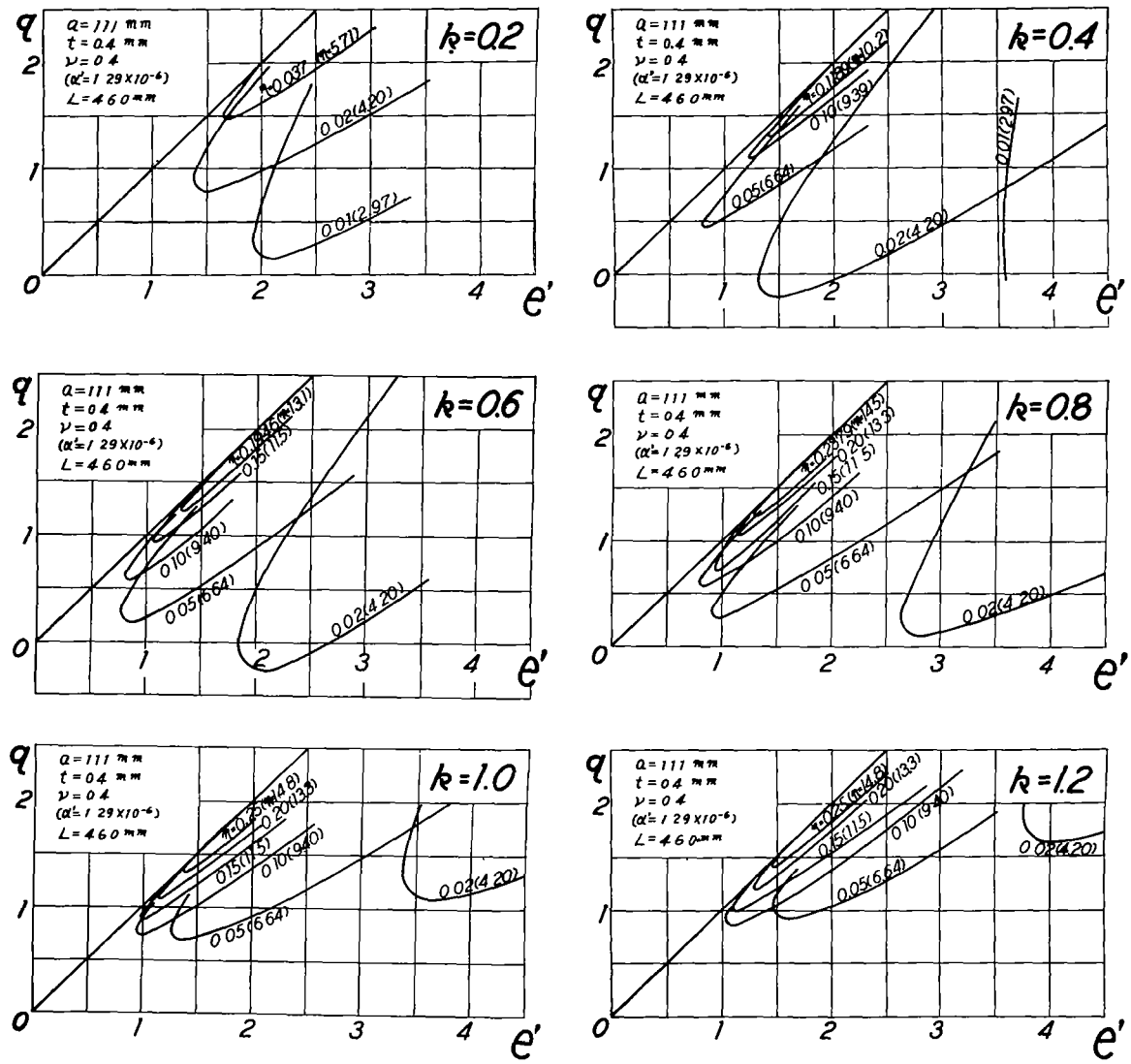

Figure 9.- Relation between the compressive stress q and unit end shortening e' for local buckling.

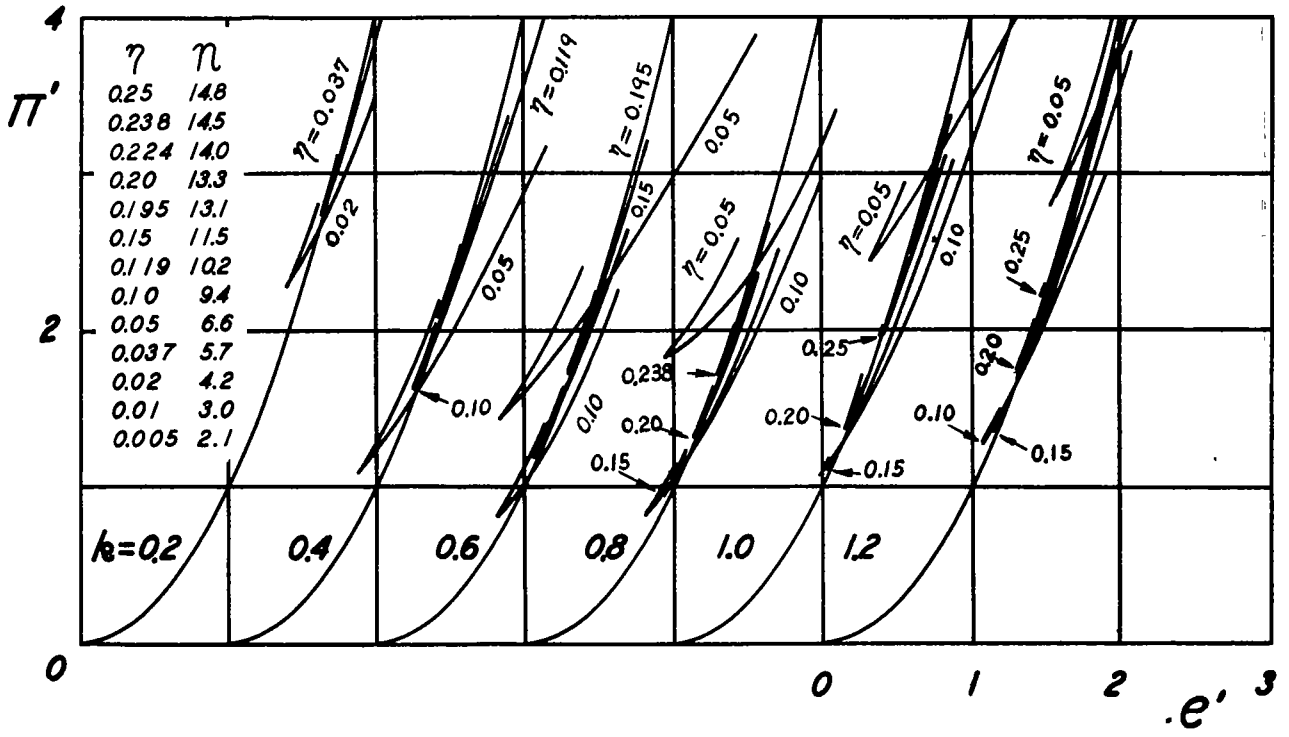

Figure 10.- Relation between the elastic energy Π' corresponding to its minimum condition with constant k and η and unit end shortening e' for local buckling.

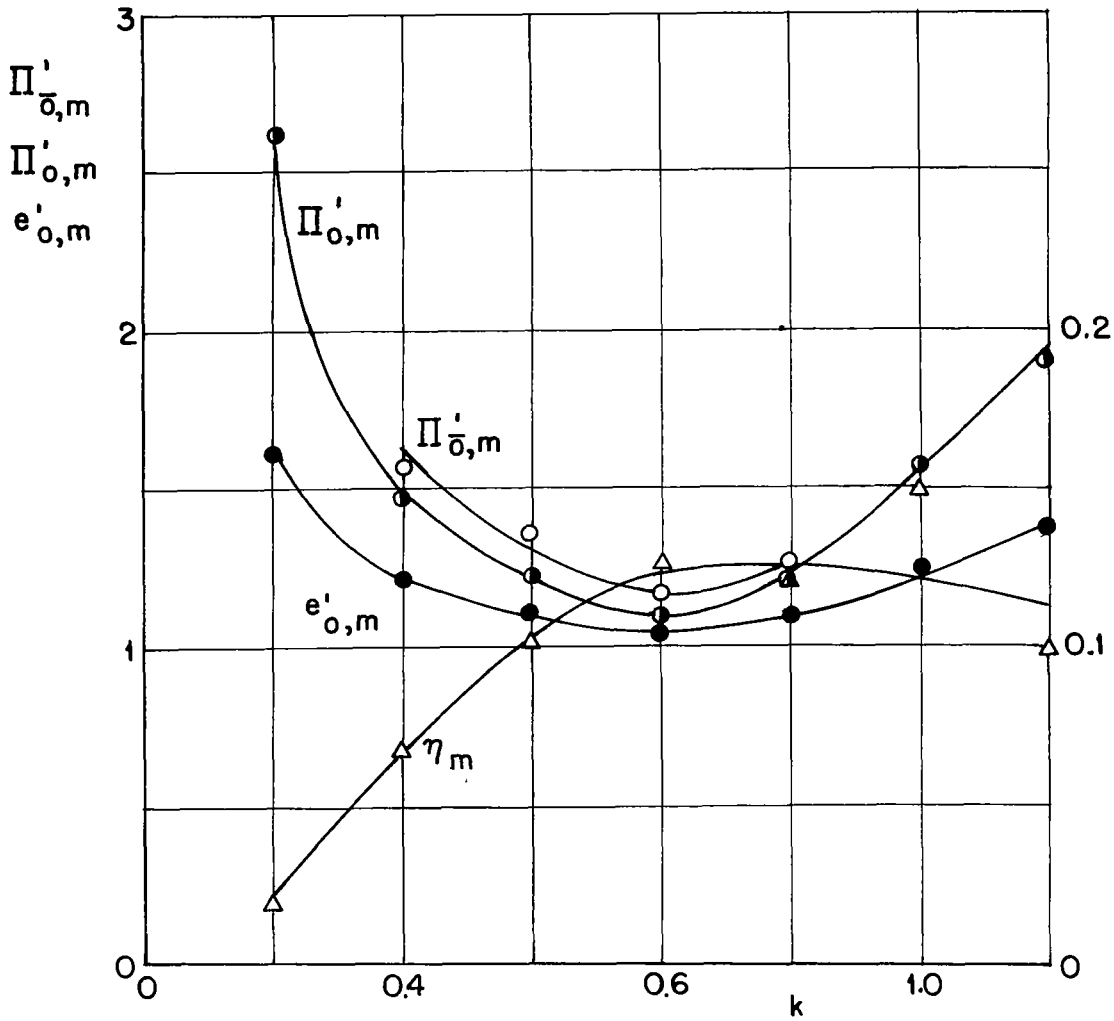

Figure 11.- Relation between the minimum $\Pi'_{o,m}$ of the elastic energy, which is equal before and after buckling, with respect to η and the aspect ratio k of the buckling lobes, for local buckling.

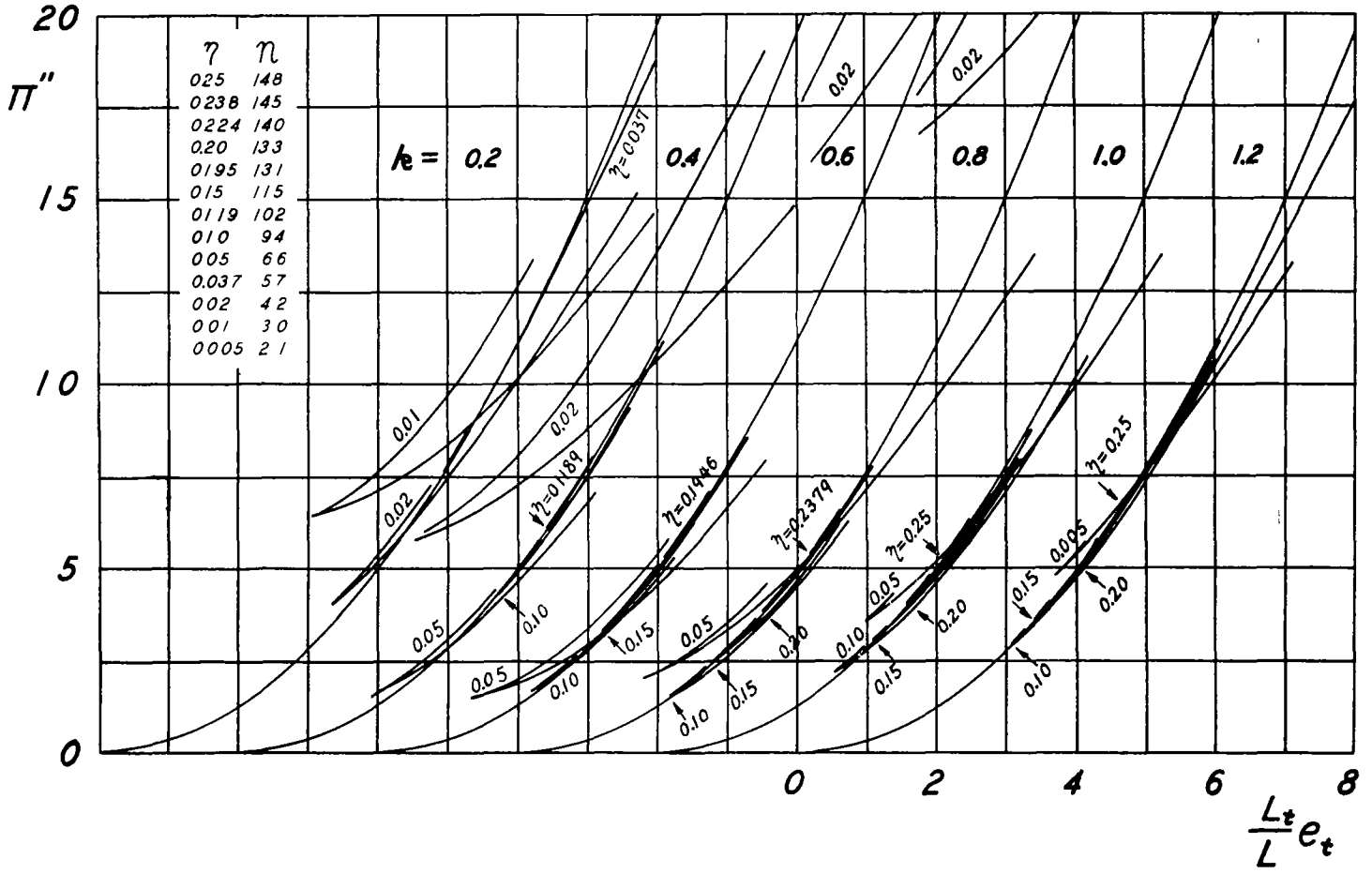

Figure 12.- Relation between the total elastic energy Π'' corresponding to its minimum condition with constant k and η and the unit end shortening e_t for local buckling of the system consisting of the shell and loading spring, the constants of which are equal to the case of experiment 2.

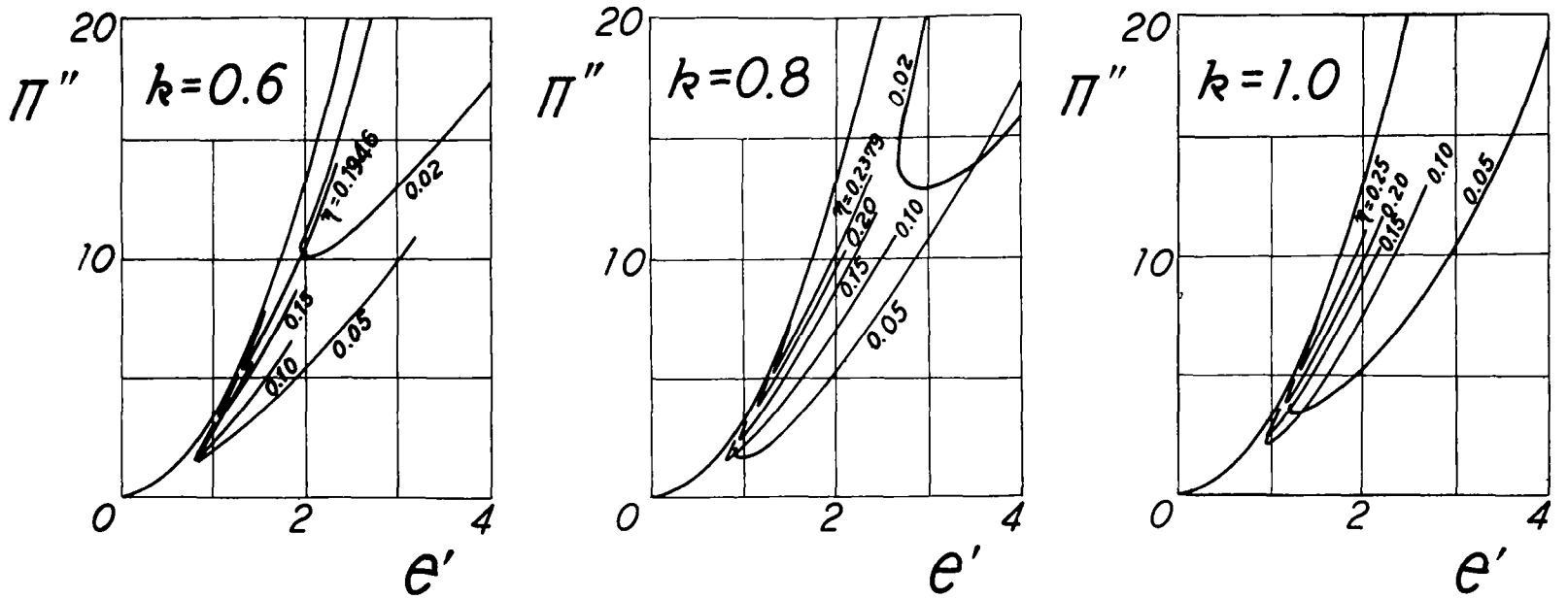

Figure 13.- Relation between the elastic energy Π'' and the unit compressive strain e' only of the shell for the case of figure 12.

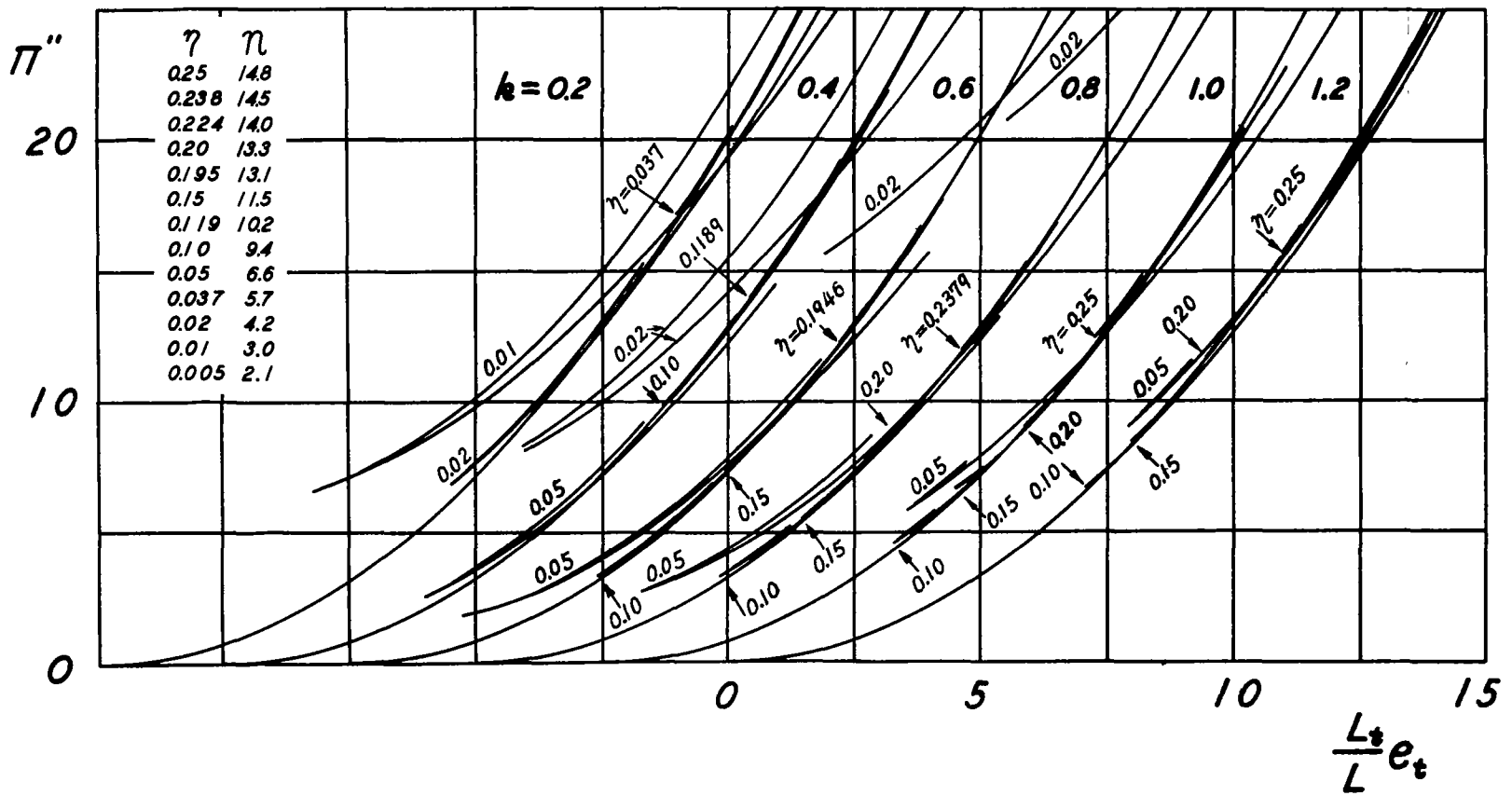

Figure 14.- Relation between the total elastic energy Π'' corresponding to its minimum condition with constant k and η and the unit end shortening e_t for local buckling of the system consisting of the shell and loading spring, the constants of which are equal to the case of experiment 3.

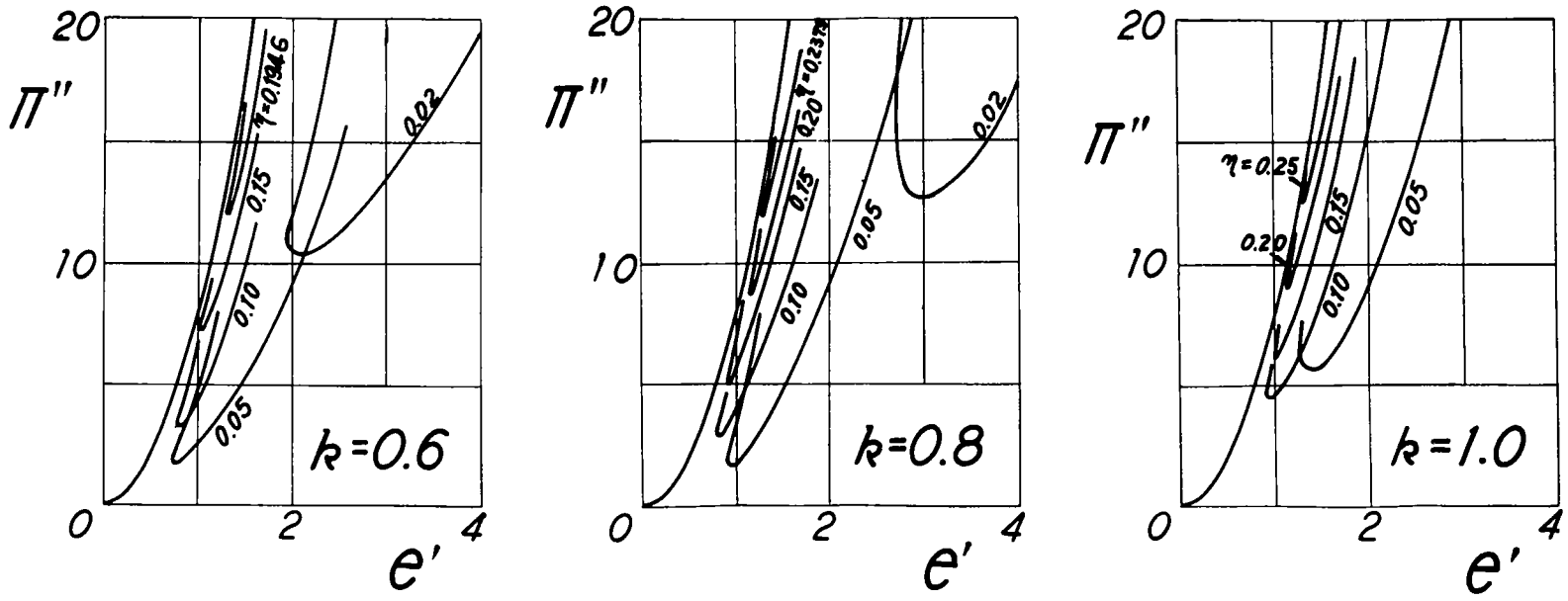

Figure 15.- Relation between the energy Π" and the unit compressive strain e' only of the shell for the case of figure 14.

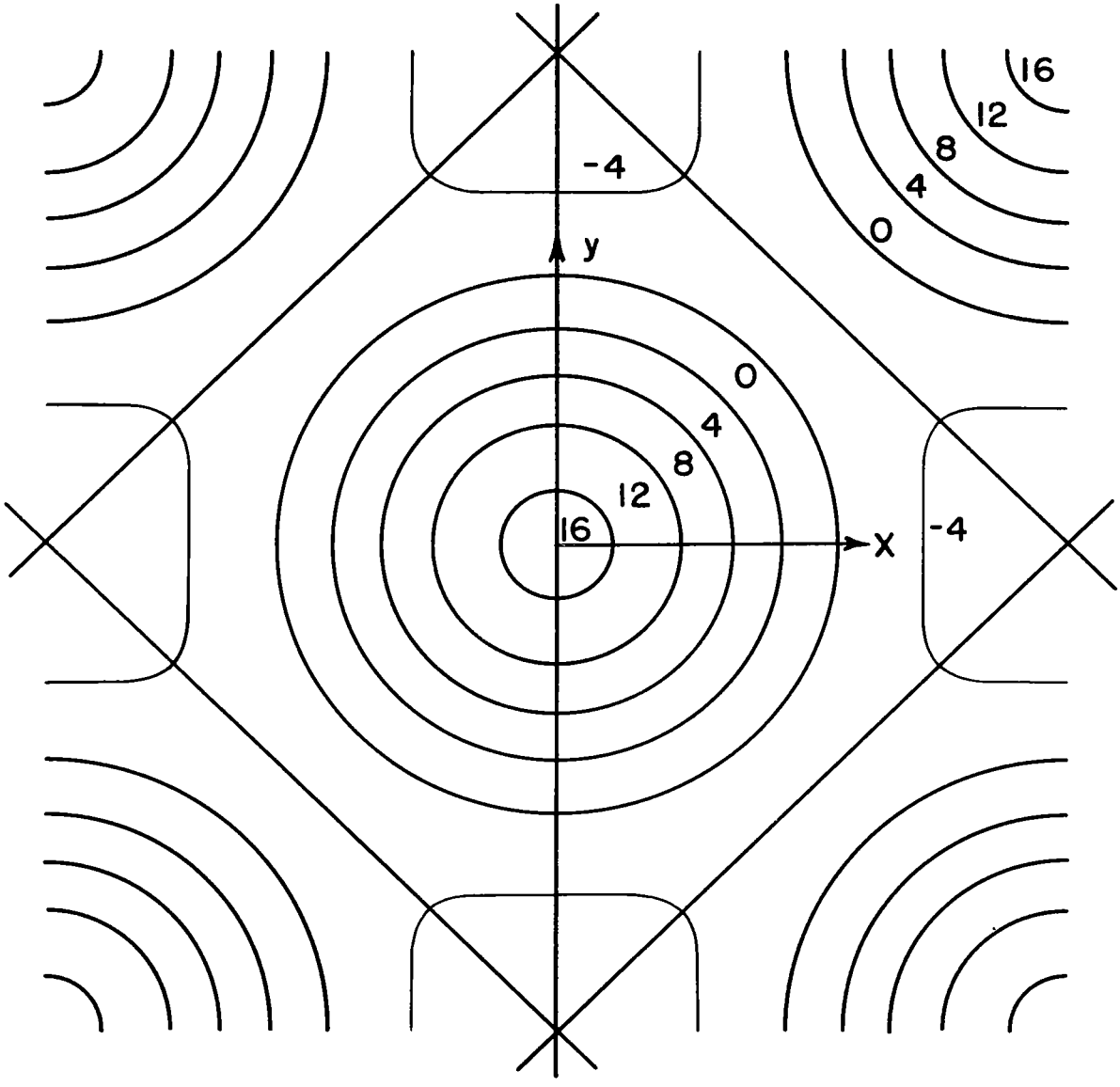

Figure 16.- Contour line of the buckled surface based on the circular cylindrical surface.

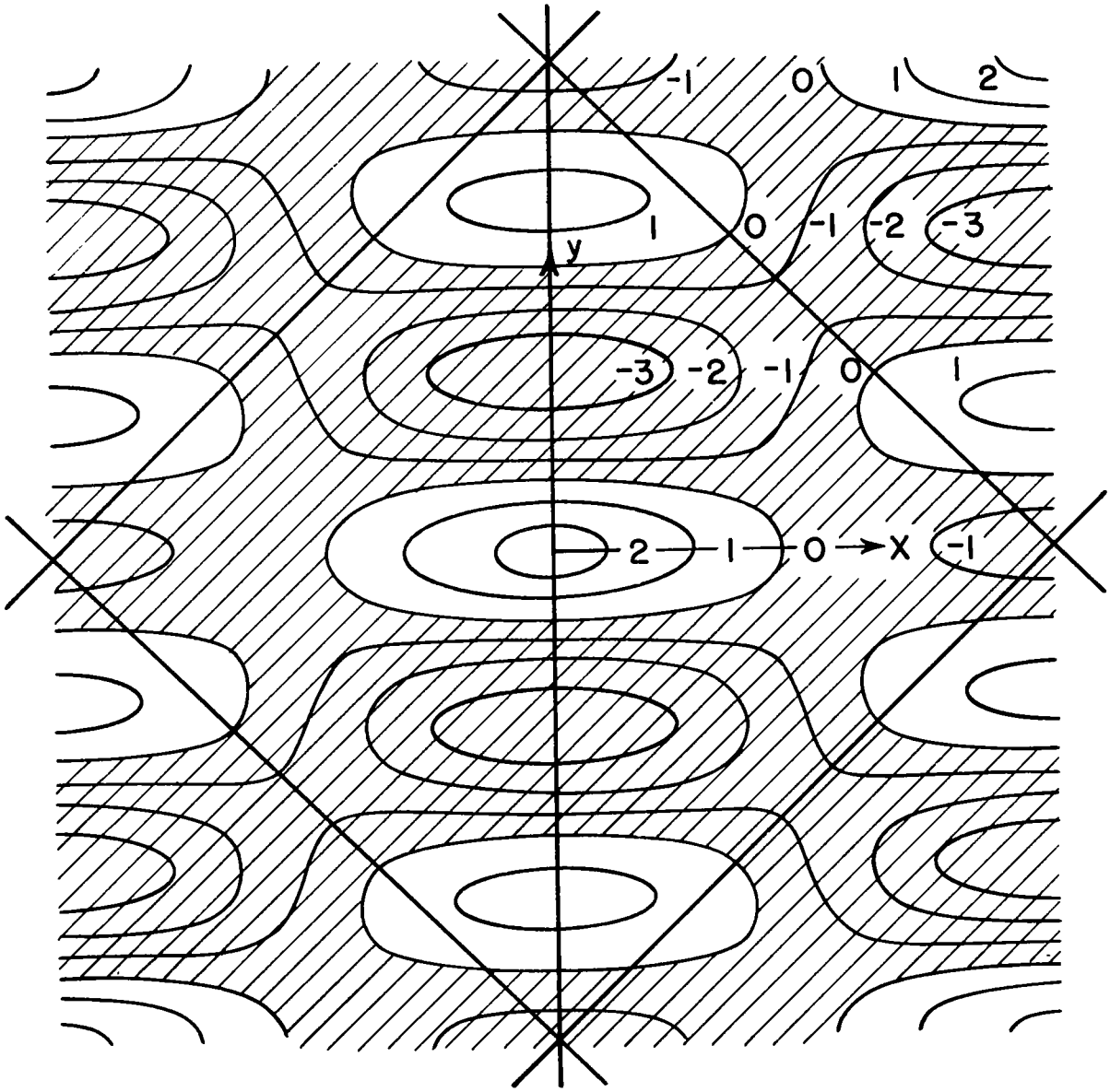

Figure 17.- Distribution of the quantity $q_x = \frac{\sigma_x}{E\sqrt{\alpha}}$, σ_x being the axial stress, negative value of which represents compression.